6-2018

# Optimization of Superhydrophobic Surface Production Using Ambient-Dried Silica-Based Aerogels

Elizabeth Donlon

# Optimization of Superhydrophobic Surface Production Using Ambient-Dried Silica-Based Aerogels

By

Elizabeth Donlon

* * * * * * * * *

Submitted in partial fulfillment
of the requirements for
Honors in the Department of Mechanical Engineering

UNION COLLEGE
June, 2018

# ABSTRACT

DONLON, ELIZABETH Optimization of Superhydrophobic Surface Production Using Ambient-Dried Silica-Based Aerogels

ADVISOR: Ann Anderson, PhD.

Superhydrophobic surfaces exhibit particular properties that make them functional in various anti-sticking, anti-contamination, self-cleaning and drag reduction applications. Though such surfaces are found in nature - most notably the lotus leaf - they are difficult to produce. There are numerous methods and techniques for fabricating superhydrophobic surfaces. One such method is the sol-gel method, in which aerogel, a highly porous and lightweight material that can be made hydrophobic or superhydrophobic, is coated onto a surface. The purpose of this project is to devise a simple and repeatable procedure for making hydrophobic silica aerogel coatings that can be used for drag reduction. Hydrophobic coatings were made using a methlytrimethoxysilane based recipe with varying amounts of methanol and water. Oxalic acid was added for hydrolysis of the precursor solution and ammonium hydroxide was used as a catalyst to form a wet-gel. The wet-gel was dissolved using methanol and the resulting homogeneous solution was applied to the surface of a microscope slide and dried at various temperatures. A Plackett-Burman experimental screening process was conducted to determine which factors in the aerogel production and coating process had the greatest effect on the quality and hydrophobicity of the coating. The application method, layers of coating, drying temperature and drying time were found to have the greatest effect on the hydrophobicity. A subsequent Randomized-Block experimental design was used to optimize the coating method and chemical recipe. Slides were coated and characterized using sessile-drop contact angle measurements, scanning electron microscopy (SEM) and surface area and porosity measurements. The highest contact angle reached was 154$^{o}$. SEM imaging shows nanometer-scale sized spherical shaped aerogel formation and an evenly coated surface.

## Table of Contents

# Table of Figures

# Table of Tables

# Chapter 1: Introduction

This chapter introduces several topics that are relevant to aerogel-based hydrophobic surfaces. It will begin with a discussion of hydrophobicity and some of the applications and methods for making superhydrophobic surfaces. It will then focus on one application – drag reduction. Following, it will discuss what aerogels are and how they can be made hydrophobic. It will then review literature pertaining to making superhydrophobic surfaces with aerogels, including the work previously done at Union College. Lastly, it will present the goals of this project.

## *1.1 Superhydrophobicity*

Wettability is a property of surfaces that defines the amount of wetting, or amount of contact between water and a solid surface. This property plays an important role in research and industry due to its various applications, as discussed further in this paper. Wettability arises from various interactions, such as intermolecular forces and acid/base chemistry, between the water and the surface. These interactions are governed by Young's law, which relates the interfacial surface-free energy between the interacting phases and contact angle by the following equation:

$$\gamma_{sg} = \gamma_{sl} + \gamma_{lg}\cos\theta$$

where $\gamma_{sg}$, $\gamma_{sl}$, and $\gamma_{lg}$ are the interfacial energies of the solid-gas, solid-liquid and liquid-gas phases respectively and $\theta$ is the contact angle [1,2]. Contact angle is the angle between the surface and the tangent of the water droplet on the surface as shown in Figure 1 [3].

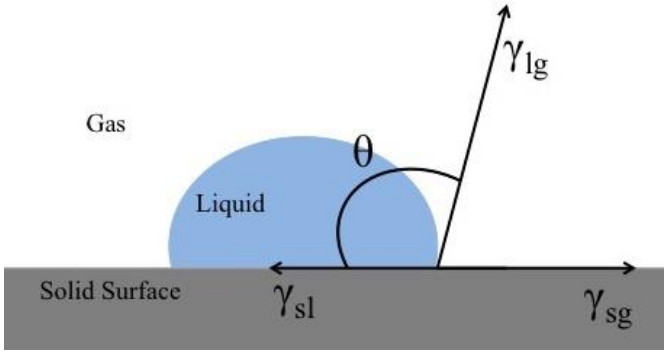


**Figure 1.** Schematic (adapted from [3]) showing contact angle, θ - the angle between the surface and the tangent of the droplet at the surface. This schematic shows a hydrophobic surface, as the contact angle is greater than 90°.

A surface with good wetting is considered hydrophilic and will have a contact angle below 90$^{o}$. Conversely, if the water is repelled by the surface causing a contact angle greater than 90$^{o}$, it is considered hydrophobic [1]. Superhydrophobicity is defined by a contact angle greater than 150$^{o}$ and is due to both intermolecular forces and surface roughness [4].

The lotus leaf is a common example of a superhydrophobic surface found in nature. These leaves, as pictured in Figure 2 [5], display a contact angle of about 160$^{o}$ [4].

**Figure 2.** Image of a lotus leaf [4]. The lotus leaf is a superhydrophobic surface that has a contact angle of about 160$^{o}$ [4].

The epicuticula wax on the lotus leaf provides low surface energy and is responsible for much of its superhydrophobic capabilities [6]. The micro and nano-scaled structure of the papilla also plays an important role in increasing the hydrophobicity. The papilla are small rounded structures, about 5-9 μm large, along the surface of the leaf [4].

This combination of surface structure and surface energy is difficult to model or replicate. Thus numerous studies have been done focusing on the variety of ways to produce superhydrophobic surfaces [7-13, 22-31]. These approaches are categorized into top-down, bottom-up and combination methods. A top-down approach carves into the surface, while a bottom-up approach adds a layer to the surface. Some methods incorporate both top-down and bottom-up techniques and are thus categorized as a combination method [1]. Examples of top-down methods include templation, photolithography and plasma treatments [7-9]. Bottom-up approaches include chemical deposition, colloidal assemblies, layer-by-layer deposition and the sol-gel method [10-11,

22-31]. Chemical vapor deposition, membrane casting, micelles and electrospinning are examples of combination methods [12-13]. Each of these methods presents their own difficulties. This study will focus on using and refining the sol-gel method. Studies focusing on this method will be discussed in detail in *Section 1.4 Literature Review*.

These surfaces are of interest because superhydrophobic materials typically display anti-sticking, anti-contamination, self-cleaning and drag reduction properties and are therefore used in a variety of applications. Superhydrophobic antifouling paints are used on boat hulls to prevent growth of marine organisms. Anti-sticking agents are used in antennas and windows to protect from snow. Anti-soiling or self-cleaning coatings are used on products such as car windshields [1]. This study is interested in the drag reduction properties and applications of superhydrophobic surfaces and thus will discuss this application in more detail in the following section.

## *1.2 Drag Reduction*

The drag reduction qualities of superhydrophobic surfaces are one of the main interests and foreseen applications of this study. This property arises from the slip that occurs on the surface of the superhydrophobic material. Typically there is a no-slip boundary condition between flow of viscous fluids and a surface, meaning the velocity of the fluid at the surface is the same as the velocity of the surface. However, there are cases in which slip occurs in flow and the velocity of the fluid is greater than that of the surface [1]. Figure 3 below shows a velocity profile for both a no-slip and slip boundary condition [14].

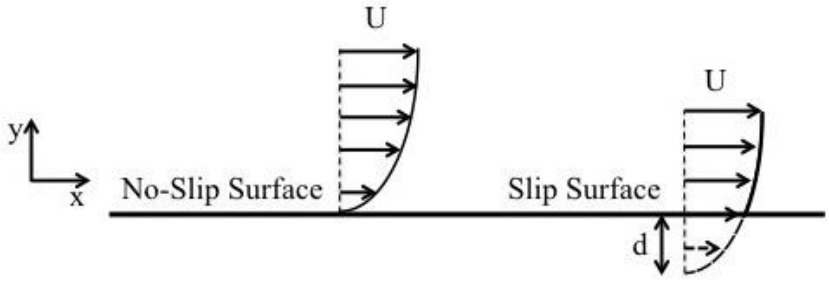


**Figure 3.** Schematic (adapted from [14]) showing velocity profiles of one-dimensional laminar flow over a flat plate with a no-slip (left) and slip (right), where U is the free stream velocity outside the boundary layer. When there is a no-slip surface, the velocity relative to the plate is zero. When there is a slip-surface, the velocity at the plate is not zero. Thus the boundary layer is smaller and drag is reduced.

As shown, when slip occurs the boundary layer and drag is reduced [14]. Slip occurs on tilted superhydrophobic surfaces because there is minimal contact between the surface and water droplet. This is why superhydrophobic surfaces have self-cleaning properties. As a water droplet rolls along the surface, it is able to pick up debris. If there was no-slip the water slides over the dust-particles and displaces them but does not collect them. This is illustrated in Figure 4 [1].

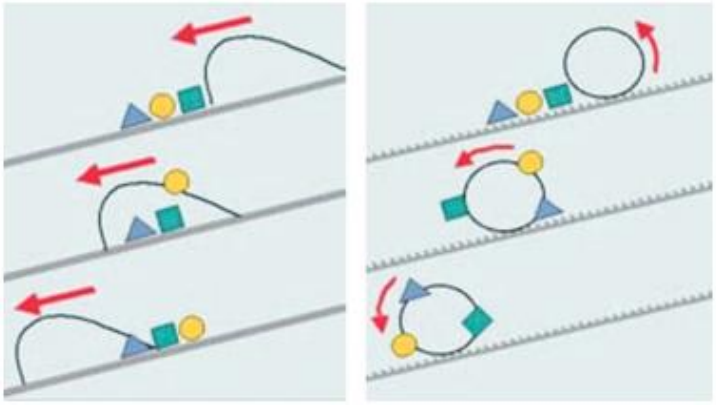

**Figure 4.** Schematic showing a water droplet moving across a no-slip hydrophobic surface (left) and a slip superhydrophobic surface (right) [1]. The arrows denote the motion of the droplet and the small shapes are debris and dust particles on the surface. The water moves over and slightly displaces the debris on the no-slip surface. The water moves over and collects the particles on the slip surface.

When slip occurs, the boundary layer is significantly reduced, as seen in Figure 3. Thus the fluid's motion is unhindered and drag is reduced [14]. To generate appreciable drag reduction, the surface slip length must be close to the characteristic length of the flow. Slip length is ratio of slip velocity to shear rate. The characteristic length of the flow is typically the length used in the Reynolds number [15]. Superhydrophobic surfaces have shown to reduce drag in both laminar and turbulent flow regimes [16].

There are several methods used to test drag or measure slip length. The methods include pressure drop experiments, velocity profile determination and force measurements [15, 17]. In pressure drop experiments, the surface is put in a channel and the drag reduction coefficient, $C_D$, is found from comparing the change in pressure over the superhydrophobic surface, $\Delta p_{SH}$, to the pressure drop over a no-slip surface, $\Delta p_{NS}$, in the same flow by the following equation [17]:

$$C_D = (\Delta p_{SH} - \Delta p_{NS})/ \Delta p_{NS}$$

Velocity profile determination is typically done using micro-particle image velocimetry (micro-PIV). This technique photographs successive images of the flow of seeded water, which is illuminated by a pulsating laser. An algorithm is then used to track each particle in the water between images, produce a velocity profile and look at how the boundary layer is affected [18]. Force measurements are taken using rheometer, which rotates a cylinder in a fluid and measures the torque on the cylinder. This torque is used to calculate the frictional drag [19].

Various studies have been completed looking at measuring drag reduction on superhydrophobic surfaces [14-19, 24-31]. A number of these studies use superhydrophobic surfaces produced using the sol-gel method and will be discussed in detail in *Section 1.4 Literature Review.*

## *1.3 Aerogels*

The sol-gel method is method used to produce aerogel substrates. Aerogels are a highly porous material, consisting of a metals and metal oxides matrix that is 90-99% air by volume. Due to their porosity, aerogels have a high surface area, low density, as well as low thermal and electrical conductivity. The sol-gel process is the formation of the solid matrix through the hydrolysis and polymerization of a precursor solution in the presence of an acid or base catalysts. This forms what is known as a sol or wet-gel, a metal or metal oxide matrix surrounded by solvent. If left to dry at ambient conditions, the pores in the matrix will collapse due to capillary tension from evaporation, forming a xerogel. To fabricate an aerogel, the solvent must be removed through supercritical extraction to keep the pores intact [20]. The schematic in Figure 5 below shows the structural difference between a wet-gel, xerogel and aerogel [21].


**Figure 5.** Schematic showing the structure of a (from left to right) wet-gel, xerogel and aerogel [21]. The purple represents the metal or metal oxide gel particles and the gray represents the solvent. In a wet-gel, solvent surrounds the metal-oxide matrix. In a xerogel the pores collapse and traps solvent within the structure. Extracting the solvent from the solid matrix of the wet-gel forms an aerogel that is 90-99% air by volume.

Silica aerogels are typically made from an alkoxide precursor solution, such as tetramethylorthosilcate (TMOS) or tetraethylorthosilcate (TEOS). These contain silica, Si, with an alkoxide group, OR. These precursors are dissolved in solvents such as methanol and water to form the colloidal particles that will make up the matrix of the sol-gel. An acid or base catalyst, such as ammonium hydroxide, $NH_4OH$, facilitates the polymerization of these particles to produce siloxane bridges of the form: ≡ Si-O-Si≡, creating the sol gel [20]. To make a superhydrophobic silica aerogels, typically methyltrimethoxysilane (MTMS) is used as the precursor or in conjunction with the other precursors. This hydrolyzed in water, methanol and oxalic acid and later polymerized with ammonia. Figure 6, shows this reaction [20].

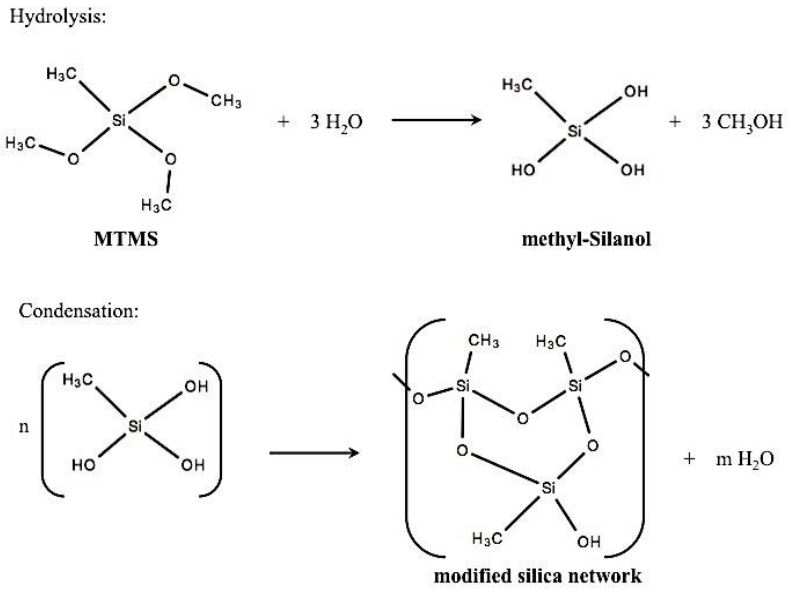


**Figure 6.** Sol-gel reaction of MTMS [20]. First hydrolysis occurs forming methyl-Silanol compounds. These then polymerize during condensation to create a silica network.

The silica aerogel is mostly made of silica, $SiO_2$. However, as shown in the silica network in Figure 6, many of the side chains remain partially or fully unreacted via hydrolysis or condensation. More specifically, the remaining alkoxide groups, in this case $SiOCH_3$ and SiOH, are completely and partially unreacted during hydrolysis. The $SiCH_3$ are left unreacted during polymerization. These side chains are at the surface of the aerogel and interact with the water. The presence of the Si-R groups, such as $SiCH_3$, will render the aerogel hydrophobic because the water has stronger intermolecular forces with itself than with these groups.

Using the sol-gel method to create superhydrophobic surfaces is an example of a bottom-up approach.

## *1.4 Literature Review*

An abundance of research on hydrophobic and superhydrophobic aerogel films has been completed [22-28].

A study conducted by Hrubesh et al. [22] focused on fabrication of thin aerogel films. These aerogels were not hydrophobic, but the methods used for coating are still applicable. The aerogel films were prepared by a precursor solution of 1:2:4:0.01 molar

ratio of tetramethoxysilane (TMOS), water, methanol, ammonium hydroxide. Oxidized metal etched and untreated glass surfaces were coated using various methods – dip coating, spin coating, spray coating and surface tension coating. The gels were supercritically dried using an autoclave. This method produced 1 to 20 μm thick aerogel films with 86%-95% porosity.

Bhagat et al. [23] studied fabrication of monolithic superhydrophobic aerogels using ambient drying. The sols were prepared by mixing MTMS, methanol and 0.01M oxalic acid. After 24 h, 10 M ammonium was added at a molar ratio of 1:8 with MTMS. The following molar ratios of MTMS to methanol were used to determine which would minimize cracking: 1:21, 1:28, 1:31.5 and 1:35. Though these aerogels were not produced as thin films, fabricating monolithic aerogel at ambient pressure is applicable. The study found that increasing the amount of methanol decreased volume shrinkage and cracking. The gels with a MTMS to methanol molar ratio of 1:35 had the least percentage volume shrinkage and were monolithic.

Budunoglu et al. [24] conducted a study on the fabrication of transparent superhydrophobic aerogel films. The films were prepared from MTMS, methanol and 0.5 mL of 0.001 M oxalic acid. The molar ratio of MTMS to methanol was varied from 1:15, 1:25 to 1:35. This was stirred for 30 min and left at room temperature for 24 h. Then 0.61 mL of 11.2 M ammonium hydroxide was added and mixed for 15 min. This was left to gel for 48 h before dissolving the gel in 10 mL of methanol with a 20 W ultrasonic liquid homogenizer for 45 s. Microscope glass slides that were previously cleaned with ethanol in a sonicator for 15 min, were spin coated with the homogenized sol-gel solution. The solution was left to dry overnight and then heated at either 450$^{o}$C or 600$^{o}$C for 1 h. The gels with a higher amount of methanol had higher contact angles of 178.4 ± 1.5$^{o}$ and 179.5 ± 0.4$^{o}$. The temperature at which they were annealed did not have a significant effect on the hydrophobicity.

Kim et al. reported studies of pressure drop in glass channels coated with superhydrophobic aerogel [25, 26]. The methods described in the papers vary slightly. In the later publishing [25], Kim et al. reports using MTMS, methanol and water in a molar ratio of 1:25:8 and 0.5 mL of 0.001 M oxalic acid to prepare the gels. The precursor solution was mixed and left for 24 h before adding 0.61 mL of 11.2 M ammonium

hydroxide. It was then aged for 48 h to form a gel. The gel was dissolved in methanol with a 100 W homogenizer for 60 s. This was injected into a glass channel and dried for 10 min and repeated 5 times at room temperature. It was then dried at 200$^{o}$C for an additional 10 min. In the previous work [26], Kim et al. did not report repeated application and drying, rather the channels were dried at 300$^{o}$C for 1 h. To measure drag, Kim et al. studied the required pressure-drop to move a droplet in the channel and related it to the viscous drag. The study found that the aerogel-coated channel had a smaller frictional force and thus less drag [25].

Fei et al. [27] also studied fabrication of transparent superhydrophobic aerogels. The gels were prepared with varying molar ratios of MTMS to methanol – 1:15, 1:20, 1:25, 1:30 and 1:35. Then 5.0 mL of 0.001 M oxalic acid was stirred in for 30 min. After 24 h, 6.1 mL of 11.2 M ammonium hydroxide was added and stirred for 15 min. This aged for 2 days before dissolving in methanol. Glass slides were coated and dried at 150$^{o}$ for 12 h. The study found that increasing the molar ratio of methanol increased the contact angle and hydrophobicity of the surface.

Rao et al [28] looked at the transport of water over superhydrophobic aerogel surfaces. The surfaces were prepared with MTMS, methanol, water and ammonium hydroxide base in varying ratios. The aerogel surfaces formed small spherical particles on the surface of the aerogel. The surface was placed on an incline and the velocity of a water droplet moving down the surface was measured using a system of LEDs and photoconductive detectors. The study concluded that structure of the surface affected the velocity of the water. The water moved faster on surfaces that formed uniform small spherical structures.

## *1.5 Prior Work at Union College*

Several students at Union College have worked on similar projects to observe flow over surfaces coated with superhydrophobic aerogel. Barabasz (ME ’11) synthesized aerogels using Union College’s patented Rapid Supercritical extraction method [29]. This method utilizes a 24-ton hot press to pressurize and heat the sol precursor solution in a mold to the supercritical point of the solvent. This allows the solvent to release as a supercritical fluid without compromising the matrix structure and

creating an aerogel in 4 to 8 hours [29]. The aerogels were powdered, mixed with Nafion, a perfluorinated ion-exchange membrane, and then painted onto glass slides. The weight percent of aerogel to Nafion was varied. The highest contact angle achieved was 160$^{o}$ with a 25% aerogel to Nafion mixture. The evenness of the coating was assessed using Scanning Electron Microscopy (SEM) imaging. Successful coatings were tested using a falling ball viscometer, rotational viscometer and micro-particle image velocimetry (micro PIV) at low Reynolds numbers. Drag reduction was not observed. Noted future work included different methods of testing to observe more significant changes in drag and flow [29].

Rodriguez (ME ’11) [30] also produced aerogels using Union College’s Rapid Supercritical Extraction method and adhered them onto surfaces using double-sided sticky tape. The amount of MTMS was varied in the precursor solution and they measured contact angles of 167°–170° for all samples. The aerogels were further characterized using Fourier transform infrared spectroscopy (IR), SEM imaging and gas adsorption. A rotational viscometer was used to observe drag in laminar flow. Drag reduction between 20–30 % was observed by all aerogel samples. This work showed that superhydrophobic aerogels are capable of effectively reducing drag. However, noted future work included creating more direct and permanent adhesion between the sol-gel and surface [30].

## *1.6 Project Objective*

The objective of this project is to produce superhydrophobic surfaces using the sol-gel method. It aims to replicate and optimize the processes found in the literature to develop a reproducible, easy and robust method. The ultimate application will be to observe the flow and drag over these surfaces. The following chapters outline the experimental method used to produce and characterize the surfaces, discuss the experimental designs used to analyze and optimize the procedure, discuss the results and concerns and presents the ideas for future work.

# Chapter 2: Experimental Methods

This chapter will first detail the process of fabricating the superhydrophobic silica aerogel films, then the method used to characterize the hydrophobicity and durability. Lastly it will review some of the preliminary experiments.

## *2.1 Aerogel Fabrication Methods*

The two-step acid-base process, consisting of hydrolysis and condensation, was used to prepare the silica sol-gels. First, 98% trimethoxymethylsilane (MTMS) was dissolved in a certain amount of methanol according to the prescribed molar ratio, either 1:25 or 1:35. Hydrolysis then occurred by adding 0.5 mL of 0.001 M oxalic acid and in some cases water at a molar ratio to MTMS of 1:8. The solution was stirred for ~2 min and then covered and left for 24 h. In the following step, 0.61 mL of 11.2 M ammonium hydroxide solution was added to the solution and stirred for ~2 min. This was covered and left for 2 days to allow for condensation to occur. The full recipe is given in Table 1.

**Table 1.** Recipe for MTMS gels for all molar ratios of MTMS:MeOH:$H_2O$

| | **Molar Ration MTMS:MeOH:$H_2O$** | | | |
|---|---|---|---|---|
| **Chemical** | **1:25:0** | **1:25:8** | **1:35:0** | **1:35:8** |
| **MTMS (mL)** | 1.00 | 1.00 | 1.00 | 1.00 |
| **MeOH (mL)** | 6.97 | 9.74 | 6.97 | 9.74 |
| **$H_2O$ (mL)** | 0 | 1.00 | 0 | 1.00 |
| **0.001 M $CH_2O_2$ (mL)** | 0.50 | 0.50 | 0.50 | 0.50 |
| **11.2 M $NH_4OH$** | 0.61 | 0.61 | 0.61 | 0.61 |

The gels were broken up and then dissolved in 10 or 30 mL of methanol and either sonicated or stirred for the prescribed amount of time.

Glass slides were prepared by first cleaning with ethanol for 5 min. Some slides were etched using sand paper and then rinsed with ethanol. An etched slide is shown in Figure 7.

**Figure 7.** Image of slide mechanically etched using sand paper.

The slides were then coating using either a dipping or pouring method. The slides that were dip-coated were placed in the solution for the prescribed amount of application time, from 1 to 15 minutes. The slides that were pour-coated were placed horizontally and the solution was poured on using a Pasteur pipette. They were then left for the prescribed amount of application time, 1 to 15 minutes. The slides were placed in a furnace at either 150ºC or 400ºC. The slides that had 5 applications were placed in the furnace for 10 min between each application. The slides were left in the furnace for either 1 h or 48 h upon the final application.

## *2.2 Contact Angle Measurements*

Hydrophobicity of the slides was measured by contact angle using a Kruss Drop Shape Analyzer (DSA 100), shown in Figure 8.

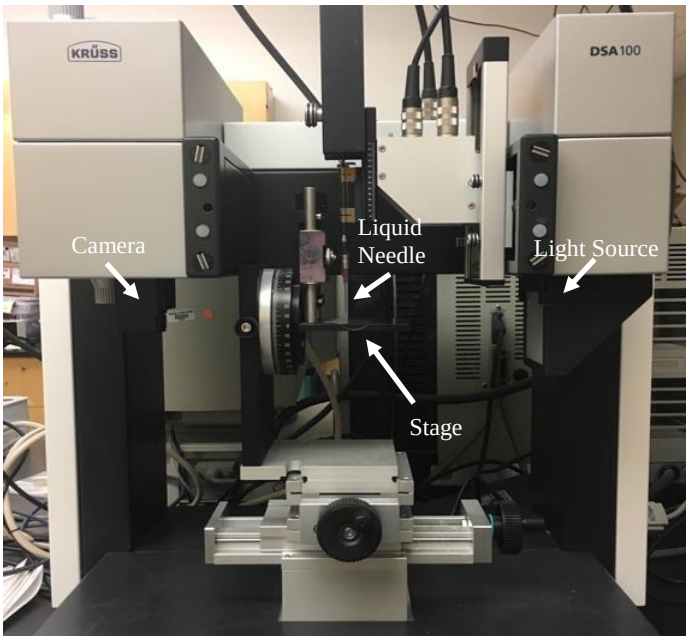


**Figure 8.** Image of Kruss Drop Shape Analyzer (DSA 100).

This instrument uses a liquid needle to place a sessile water droplet of specified size onto the surface. The drop is imaged and the contact angle is measured from the three-phase contact points between the baseline and contour of the drop surface using the Tangent method, as shown in Figure 9.

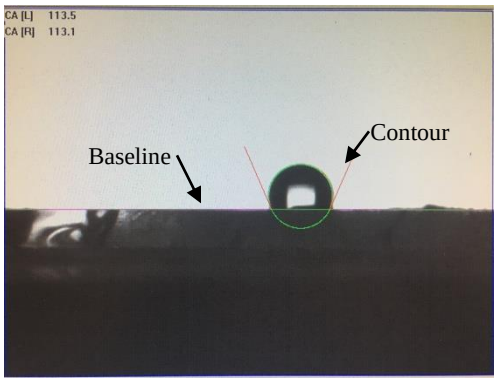


**Figure 9.** Image of drop contact angle measurement with Kruss Drop Shape Analyzer. The baseline (blue) is determined manually and the analyzer determines the contour (green) of the drop and measures with the Tangent Method the left and right contact angle with from the tangent of the drop at the baseline.

A total of 10 contact angle measurements were made on each slide using 2 μL-sized drops placed at various locations. For a table of all contact angle measurements, please refer to Appendix A – Contact angle measurements.

## *2.3 SEM*

A Zeiss EVO 50XVP Scanning electron microscope (SEM), shown in Figure 10, was used to obtain photos of the surfaces at a micro and nano-scale.


**Figure 10.** Image of Union College Zeiss EVO 50XVP SEM.

The microscope was used in Secondary Electron Mode with a spot size of 380-430 and an extra high tension (EHT) voltage of 8-15 kV. These images are useful for assessing the quality, evenness and structure of the surface coating.

## *2.4 Water Testing*

It is important that these surfaces are durable enough to actually be used in water. Therefore two forms of water testing were done on selected slides to determine the robustness of the coating in water. The first form was extended water exposure. The slides were submerged in water for 24 hours. Contact angle measurements were made before and after the test to determine whether the surface was affected. The second form of water testing was running water exposure. The slides were placed under running water for 1 minute. Again, contact angle measurements were taken before and after to see if the surface could withstand the running water.

## *2.5 Preliminary Experiments*

Preliminary work focused on trying to repeat the experimental procedure from Kim et al. [25] described in *Section 1.4 Literature Review.* This procedure was followed twice using 150 mL and 30 mL of methanol to dissolve the gel, as the amount was not specified in Kim et al.'s study. The solutions were sonicated several times and stirred with a stir bar. However, in both cases the gels did not dissolve, as shown in Figure 11.

**Figure 11.** Image of attempts to dissolve sol-gel in methanol following the procedure from Kim et al. [25]. The gel did not complete dissolve, most of it collected at the bottom of the beaker.

As an adaptation of the methods used by Kim et al., methanol was added to aerogels made at Union College in 2013 by Yi Cao '15 using RSCE method. These aerogels were

made using TMOS silica aerogels with 25%, 50% and 75% MTMS. The recipe used to make these gels is described in *Section 6.3 MTMS Study*. Theses were crushed into pieces about 2-5 mm in diameter, as show in Figure 12.

**Figure 12.** Image of crushed aerogels made by Yi Cao '15 at Union College using the RSCE method in 2013, made with (from left to right) 25%, 50% and 75% MTMS.

Next, 70 mL of methanol was added to the 25% and 50% MTMS aerogels and 115 mL of methanol was added to the 75% MTMS aerogel. More methanol was used for the 75% MTMS aerogel because it appeared to dissolve less. As shown, in Figure 13, the aerogels appear at the bottom of the solution.

**Figure 13.** Image of (from left to right) 25% and 50% MTMS aerogels dissolved in 70 mL of methanol and the 75% MTMS aerogel dissolved in 115 mL of methanol. The aerogel dissolved slightly, but appears to mostly sit at the bottom of the beaker.

Glass slides were dipped into the gel and placed in an oven at 200$^{o}$C for 10 min. This was repeated 5 times. The slides did not coat and were not hydrophobic, as show in Figure 14.

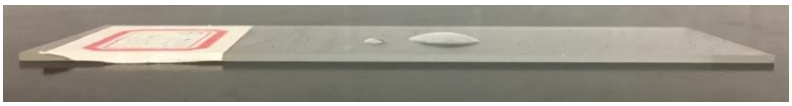

**Figure 14.** Image of water drop on 75% TEOS aerogel coated glass slide. The slide does not appear to have any coating on it and the water clearly adheres to the surface, thus it is not hydrophobic.

This procedure was repeated using 10 mL of methanol to dissolve each, as shown in Figure 15.

**Figure 15.** Image of slurry made with (from left to right) 25%, 50% and 75% MTMS aerogels in 10 mL of methanol.

Glass slides were soaked in the gel for 1 min before placing in an oven at 300$^{o}$C for 10 min. This was repeated 5 times. The gels again did not appear to coat the slides.

These preliminary experiments showed that there were several factors that could affect the quality of the aerogel film, including amount of methanol used to dissolve and homogenizing method. Though the techniques used in the literature are similar, the slight distinctions could affect on the results. Therefore a Plackett-Burman screening process was used to determine which factors most affect the hydrophobicity of the coatings. The following chapter will discuss the experimental set-up and design of the screening test.

# Chapter 3: Plackett-Burman Screening

This chapter will discuss the Plackett-Burman Experimental Screening process that was conducted to optimize the superhydrophobic surfaces. The chapter will begin by describing what a Plackett-Burman Experimental Screening process entails and how it was applied to this study. Finally it will review the results and conclusions. In the following sections each slide will be referred to by ED-MTMS-## where ED is the experimenters initials, MTMS is the precursor used, and ## is the experiment number from the Plackett-Burman Design.

## *3.1 Plackett-Burman Screening Method*

A Plackett-Burman Screening process was employed to determine which factors in the superhydrophobic surface production process have the greatest effect on the hydrophobicity. The Plackett-Burman method is used to determine the effect of different factors. This design uses 4*n* experiments, where *n* is any integer and 4*n*-1 is equal to the number of factors that may be influencing the results. Thus, if there are 11 factors influencing the results, 12 experiments will be conducted. This is a two-level factor design, meaning each factor is given a high and a low value. This "value" can be quantitative or qualitative [32]. Each experiment is conducted using the high or low value for each factor according to the Plackett-Burman matrix, shown in Table 2.

**Table 2**. Plackett-Burman 12-experiment Matrix. Note that + denote high values and – denote low values for each factor. Factors are represented by a letter, A-K.

| | Factors | | | | | | | | | | | |
|---|---|---|---|---|---|---|---|---|---|---|---|---|
| **Experiment** | **A** | **B** | **C** | **D** | **E** | **F** | **G** | **H** | **J** | **K** | **L** | **Result** |
| **1** | + | + | + | + | + | + | + | + | + | + | + | $y_1$ |
| **2** | + | + | + | + | - | - | - | + | - | - | - | $y_2$ |
| **3** | + | + | - | - | - | + | - | - | + | - | + | $y_3$ |
| **4** | + | - | + | - | + | + | + | - | - | - | - | $y_4$ |
| **5** | + | - | - | + | - | - | + | - | + | + | - | $y_5$ |
| **6** | + | - | - | - | + | - | - | + | - | + | + | $y_6$ |
| **7** | - | + | + | - | - | - | + | - | - | + | + | $y_7$ |
| **8** | - | + | - | + | + | + | - | - | - | + | - | $y_8$ |
| **9** | - | + | - | - | + | - | + | + | + | - | - | $y_9$ |
| **10** | - | - | + | + | + | - | - | - | + | - | + | $y_{10}$ |
| **11** | - | - | + | - | - | + | - | + | + | + | - | $y_{11}$ |
| **12** | - | - | - | + | - | + | + | + | - | - | + | $y_{12}$ |
| **Effect** | $2[\Sigma(y_n+)- \Sigma(y_n-)]/N$ | | | | | | | | | | | |

This matrix is for a 12-experiment design. The high values are represented by a + and low values are represented by a -. Each factor is denoted by a letter, A-L.

After each experiment is completed, a result, $y_n$, must be obtained, where n is the number experiment. The effect of each factor is then estimated using the following equation:

$$\text{Effect} = 2[\Sigma(y_n+)- \Sigma(y_n-)]/N$$

where N is the total number of experiments and $y_n+$ are the $y_n-$ values for each experiment using the high value and $y_n-$ is the $y_n$ values for each experiment using the low value. The effect coefficient communicates the effect of that factor; the greater the absolute value of coefficient the greater the effect. If the coefficient is negative then as that factor is decreased the greater the affect it has. Similarly if it is positive, the effect is increased as that factor is increased [32].

The sum of squares, SS, can then be found using the following equation:

$$SS = N(\text{effect})^2/4$$

in order to estimate the error in each effect [32].

## *3.2 Experimental Design*

In this study the following factors were used in a 12-experiment Plackett-Burman Screening test: slide preparation, molar ratio of MTMS to methanol, molar ratio of MTMS to water, amount of methanol used to dissolve sol, homogenizing time, homogenizing method, coating application method, number of applications, length of applied time, drying temperature, and drying time. These factors were determined from the variations in procedures from the literature. The high and low values of each factor were determined from literature and availability of resources. Table 3 lists each factor with its high and low value, and the assigned letter to be used in a Plackett-Burman matrix.

**Table 3.** List of factors for Plackett-Burman 12-experiment screening test and high (+) and low (-) values.

| **Factor** | **Letter** | **-** | **+** |
|---|---|---|---|
| Slide preparation | A | Clean with ethanol | Etch |
| Molar ratio MTMS:MeOH | B | 1:25 | 1:35 |
| Molar ratio MTMS:$H_2O$ | C | 1:00 | 1:08 |
| Amount of methanol dissolving | D | 10 mL | 30 mL |
| Homogenizing Time | E | 45 s | 5 min |
| Homogenizing Method | F | Sonication | Stir bar and stir plate |
| Application Method | G | Dip | Pour |
| Number of applications | H | 1 | 5 |
| Application time | J | 1 min | 10 min |
| Drying temperature | K | 150$^o$C | 400$^o$C |
| Drying time | L | 1 h | 48 h |

The result for the design is contact angle, as this quantifies hydrophobicity. Table 4 summarizes the procedure used to prepare each slide in the Plackett-Burman screening process.

**Table 4.** Precursor molar ratio, dissolving method, slide preparation, application method and drying procedure for each sample based on the Plackett-Burman experimental design.

| | | Sol Dissolving | | | | Application Method | | | Drying | |
|---|---|---|---|---|---|---|---|---|---|---|
| **Sample** | **Molar Ratio (MTMS:MeOH:$H_2O$)** | **Amount of MeOH (mL)** | **Homogenizing Method** | **Time** | **Slide preparation** | **Coating Method** | **Number of Applications** | **Time (min)** | **Temp (ºC)** | **Time (h)** |
| ED-MTMS-01 | 1:25:0 | 10 | Sonication | 45 s | Cleaned | Dip | 1 | 1 | 150 | 1 |
| ED-MTMS-02 | 1:25:0 | 10 | Stir | 5 min | Cleaned | Pour | 1 | 10 | 400 | 48 |
| ED-MTMS-03 | 1:25:8 | 30 | Sonication | 5 min | Cleaned | Pour | 5 | 1 | 400 | 1 |
| ED-MTMS-04 | 1:35:0 | 30 | Sonication | 45 s | Cleaned | Dip | 5 | 10 | 400 | 48 |
| ED-MTMS-05 | 1:35:8 | 10 | Sonication | 5 min | Cleaned | Dip | 5 | 1 | 150 | 48 |
| ED-MTMS-06 | 1:35:8 | 30 | Stir | 45 s | Cleaned | Pour | 1 | 1 | 150 | 1 |
| ED-MTMS-07 | 1:25:0 | 30 | Stir | 5 min | Etched | Dip | 5 | 10 | 150 | 1 |
| ED-MTMS-08 | 1:25:8 | 10 | Sonication | 45 s | Etched | Pour | 5 | 10 | 150 | 48 |
| ED-MTMS-09 | 1:25:8 | 30 | Stir | 45 s | Etched | Dip | 1 | 1 | 400 | 48 |
| ED-MTMS-10 | 1:35:0 | 10 | Stir | 45 s | Etched | Pour | 5 | 1 | 400 | 1 |
| ED-MTMS-11 | 1:35:0 | 30 | Stir | 5 min | Etched | Pour | 1 | 1 | 150 | 48 |
| ED-MTMS-12 | 1:35:8 | 10 | Sonication | 5 min | Etched | Dip | 1 | 10 | 400 | 1 |

## *3.4 Results and Discussion*

### 3.4a Qualitative Results

The sol-gels for each experiment in the Plackett-Burman screening process were successfully synthesized. The gels were turned into a slurry according to the procedure outlined in *Section 2.1 Aerogel Fabrication Methods*. Available images of the slurries and key observations for each are summarized in Table 5. The gels that were stirred or sonicated for 5 min appeared to be more homogenous than those only stirred or sonicated for 45 s. Stirring broke up the gel into chunks, while sonication created more homogenous slurries. The slides dissolved in 30 mL of liquid often had excess liquid. The slides dissolved in 10 mL of methanol were thicker and more gel like.

**Table 5.** Images, brief description of procedure and key observations of slurries.

| Experiment | Brief Procedure | Key Observations | Image |
|---|---|---|---|
| ED-MTMS-01 | 10 mL of methanol Sonicated for 45 s | Homogenous slurry | N/A |
| ED-MTMS-02 | 10 mL of methanol stirred for 5 min | Chunky slurry | N/A |
| ED-MTMS-03 | 30 mL of methanol sonicated for 5 min | Chunks of slurry/gel with excess liquid | N/A |
| ED-MTMS-04 | 30 mL of methanol Sonicated for 45 s | Chunks of slurry/gel with excess liquid | N/A |
| ED-MTMS-05 | 10 mL of methanol sonicated for 5 min | Homogenous slurry |  |
| ED-MTMS-06 | 30 mL of methanol stirred for 45 s | Large chunks of gel in methanol Not well combined |  |
| ED-MTMS-07 | 30 mL of methanol stirred for 5 min | Fairly homogenous liquid |  |
| ED-MTMS-08 | 10 mL of methanol sonicated for 45 s | Very gel like Still able use Pasture Pipette |  |
| ED-MTMS-09 | 30 mL of methanol stirred for 45 s | Large chunks of gel Not well combined | N/A |
| ED-MTMS-10 | 10 mL of methanol stirred for 45 s | Very gel like Still able use Pasture Pipette | N/A |
| ED-MTMS-11 | 30 mL of methanol stirred for 5 min | Fairly homogenous liquid |  |
| ED-MTMS-12 | 10 mL of methanol sonicated for 5 min | Homogenous slurry | N/A |

The slides were prepared and coated according to the procedure outlined in *Section 2.1 Aerogel Fabrication Methods*. Contact angle measurements were made on all slides. Table 6 includes key observations, images of all slides, average contact angle measurements and an image of a drop on each slide for the highest contact angle measured.

The pouring method made sturdier and evener coatings than the dip coating method. The slides dried at 400$^{o}$C had flakier coatings. ED-MTMS-03, ED-MTMS-10 and ED-MTMS-04 shattered when the gel was applied to the surface because of the high temperature of the glass and the colder gel. Thus this temperature is not effective. The gels that were applied multiple times appeared to have thicker coatings, however were flakier. Some of the coatings, ED-MTMS-02, ED-MTMS-08 and ED-MTMS-10 were hydrophobic, the water droplet would not stick to the slide. The droplet was either increased in size or dropped onto the slide. The water droplets appeared to shrink as they sat on the slides, meaning the water may be penetrating the surface.

**Table 6.** Brief description of procedure, key observations, images, average contact angle and highest contact angle image of coated slides. Contact angles are reported as the average with the standard deviation for 10 measurements.

| Experiment | Brief Procedure | Key Observations | Image | Avg. CA (º) | CA image |
|---|---|---|---|---|---|
| ED-MTMS-01 | Slide cleaned<br>Pour coated<br>1 application,<br>1 min | Extremely light coating. |  | 90.5 ± 4.8 | 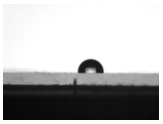 |
| ED-MTMS-02 | Slide cleaned<br>Pour coated<br>1 application,<br>10 min | Thin, uneven coating. Variations in hydrophobicity along slide | 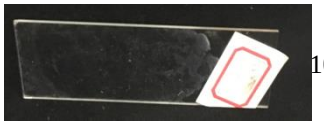 | 106.7 ± 12.9 | 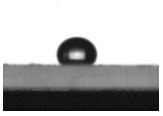 |
| ED-MTMS-03 | Slide cleaned<br>Pour coated<br>5 applications,<br>1 min | Glass shattered during reapplication due to high temperatures. Coating flaked off |  | 22.2 ± 12.6 | 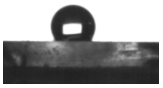 |
| ED-MTMS-04 | Slide cleaned<br>Dip coated<br>5 applications,<br>10 min | Glass shattered during reapplication due to high temperatures. Light, dusty coating. |  | 41.2 ± 10.4 | 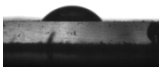 |
| ED-MTMS-05 | Slide cleaned<br>Dip coated<br>5 applications,<br>1 min | Uneven light coating |  | 87.4 ± 2.8 | 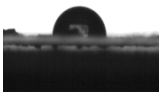 |
| ED-MTMS-06 | Slide cleaned<br>Pour coated<br>1 application,<br>1 min | Uneven light coating | 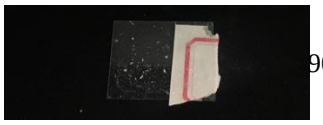 | 90.1 ± 5.9 | 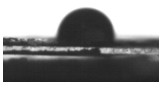 |
| ED-MTMS-07 | Slide etched<br>Dip coated<br>5 applications,<br>10 min | Even, thin coating |  | 100.7 ± 9.3 | 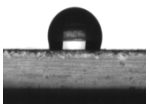 |
| ED-MTMS-08 | Slide etched<br>Pour coated<br>5 applications,<br>10 min | Thick coating. Some dusting. Had to increase droplet size for some measurements. |  | 132.8 ± 7.3 | 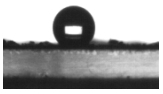 |
| ED-MTMS-09 | Slide etched<br>Dip coated<br>1 application,<br>1 min | Uneven light coating |  | 111.0 ± 11.9 | 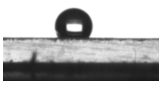 |
| ED-MTMS-10 | Slide etched<br>Pour coated<br>5 applications,<br>1 min | Glass shattered during reapplication due to high temperatures. Coating even. |  | 128.6 ± 14.3 | 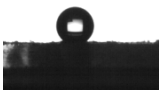 |
| ED-MTMS-11 | Slide etched<br>Pour coated<br>1 application,<br>1 min | Uneven light coating | 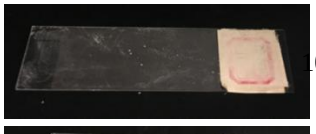 | 104.4 ± 5.7 | 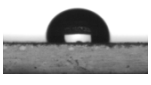 |
| ED-MTMS-12 | Slide Etched<br>Dip Coated<br>1 application<br>10 min | Hardly coated. Hydrophilic |  | 54.5 ± 5.3 | 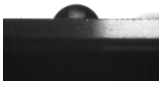 |

3.4b SEM Imaging

SEM imaging was used for closer observations of the coatings of ED-MTMS-08, ED-MTMS-02 and ED-MTMS-10, as these slides had some of the better contact angle results.

SEM images of ED-MTMS-02, shown in Figure 16, show uneven aerogel coating with some larger chunks along the surface. The aerogel on the surface has the typical "feathery" or cloud-like appearance usually seen by aerogels.

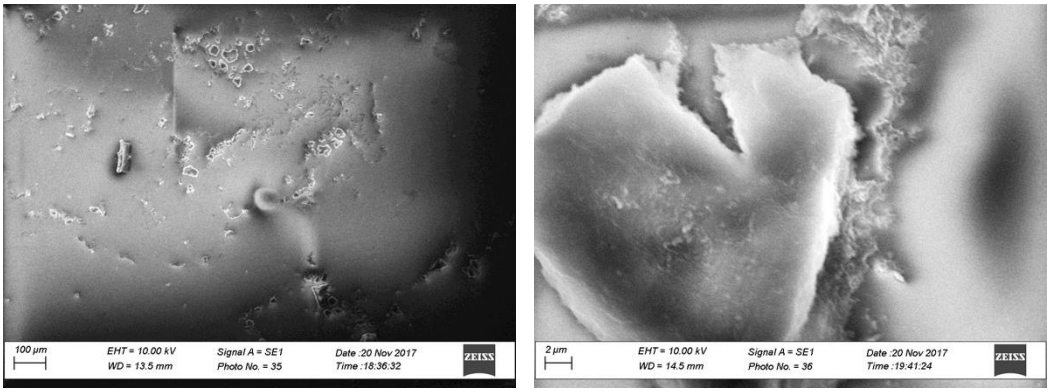


**Figure 16.** SEM imaging of ED-MTMS-02 at 100 µm (left) and 2 µm (right) scale. As shown in the left image, the left side of the slide has thin aerogel coating. However is no evenly distributed. There are chunks of aerogel scattered along the surface. The right image shows a close up of one of these particles.

Figure 17 shows SEM images of ED-MTMS-08. The aerogel on these slides are small, spherical beads. This is atypical of aerogel structure. Surface-roughness contributes to superhydrophobicity. Thus this structure could increase the hydrophobicity of the surface. The coating is fairly even over the slide, with some small holes in the coating.

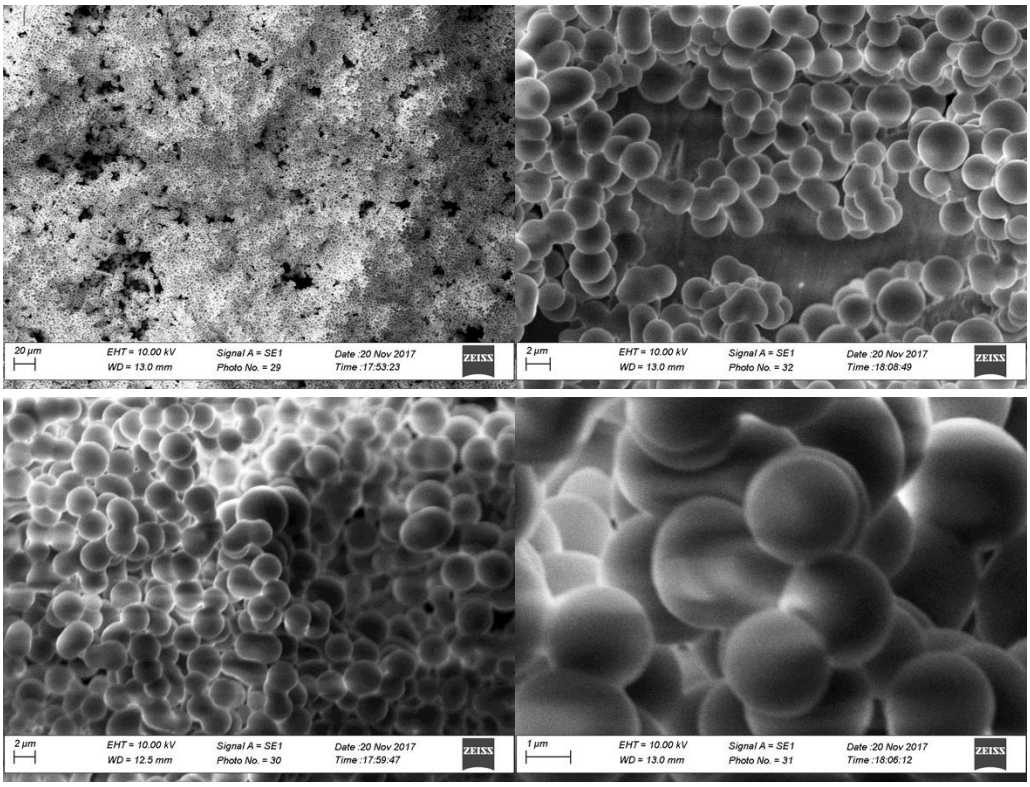


**Figure 17.** SEM imaging of ED-MTMS-08 at 20 µm (left-top), 2 µm (right-top, left-bottom) and 1 µm scale. As shown in the top two images, the coating is fairly even along the surface of the slide, with some gaps. The aerogel formed small spherical beads.

SEM images of ED-MTMS-10 are given in Figure 18. These show a thin layer of feathery aerogel like coating along the surface. This coating is uneven, with large gaps between areas of coating. This coating does not have as many chunks of aerogel along the surface.

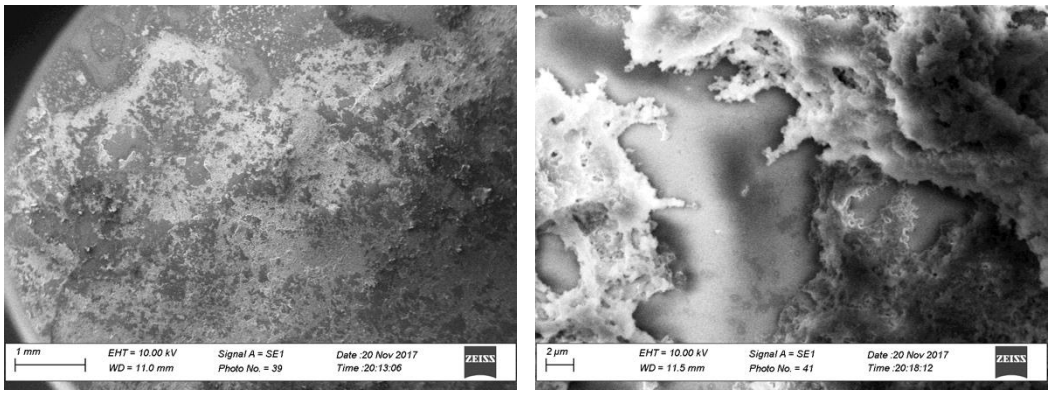


**Figure 18.** SEM imaging of ED-MTMS-10 at 1 mm (left), 2 µm (right) and 1 µm scale. As shown in the left image, there is a thin, uneven coating. The right image shows a feather like structure to the aerogel.

3.4c Water Testing Results

Two slides, ED-MTMS-08 and ED-MTMS-10, were subjected to water testing as described in *Section 2.4 Water Testing*. Images of the surfaces during extended water exposure are shown in Figure 19.

**Figure 19.** Images of ED-MTMS-08 (left) and ED-MTMS-10 (right) during extended water exposure. Note that the black dot appearing on the slide is due to the sticker used in mounting for SEM imaging.

During initial submersion, some aerogel appeared to flake off the surface and float in the water. However, no more aerogel appeared to come off during extended water exposure or running water exposure. Images of the slides after water testing are shown in Figure 20.

**Figure 20.** Images of ED-MTMS-08 (left) and ED-MTMS-10 (right) after water testing. Note that the black dot appearing on the slide is due to the sticker used in mounting for SEM imaging.

The contact angles measured before and after water testing are listed in Table 7.

**Table 7**. Average and standard deviation of contact angle from 10 measurements before and after water testing

| Slide | Before | After |
|---|---|---|
| ED-MTMS-08 | 132.8 ± 7.3 | 137.4 ± 7.8 |
| ED-MTMS-10 | 128.6 ± 14.3 | 119.4 ±11.8 |

The contact angle did not change, within standard deviation, after water testing. Therefore the coatings on ED-MTMS-08 and ED-MTMS-10 are durable enough to be used in water.

3.4d Plackett-Burman Results

The contact angle was used as the result in the Plackett-Burman screening analysis to find the effect and the sum of squares, as described in *Section 3.1 Plackett-Burman Screening Method* for each factor. Table 8 summarizes the results of the Plackett-Burman Screening.

**Table 8**. Results from Plackett-Burman 12-experiment Design.

| | | Result | | |
|---|---|---|---|---|
| | **Factor** | **CA (º)** | **Effect** | **SS** |
| **A** | Slide Preparation | 90.5 | 15.650 | 734.77 |
| **B** | MTMS:MeOH | 106.7 | -26.28 | 2072.44 |
| **C** | MTMS:Water | 122.2 | 4.317 | 55.90 |
| **D** | Amount of MeOH | 41.2 | -5.150 | 79.57 |
| **E** | Homogenizing Time | 87.4 | -3.050 | 27.91 |
| **F** | Homogenizing Method | 90.1 | 13.150 | 518.77 |
| **G** | Application Method | 100.7 | 33.25 | 3316.69 |
| **H** | Number of Applications | 132.8 | 9.283 | 258.54 |
| **J** | Application Time | 111.0 | -19.683 | 1162.30 |
| **K** | Drying Temperature | 128.6 | -6.950 | 144.91 |
| **L** | Drying Time | 104.4 | -0.5167 | 0.80 |

The Pareto Chart in Figure 21 below shows the absolute value of the effects to compare the significance of each factor.

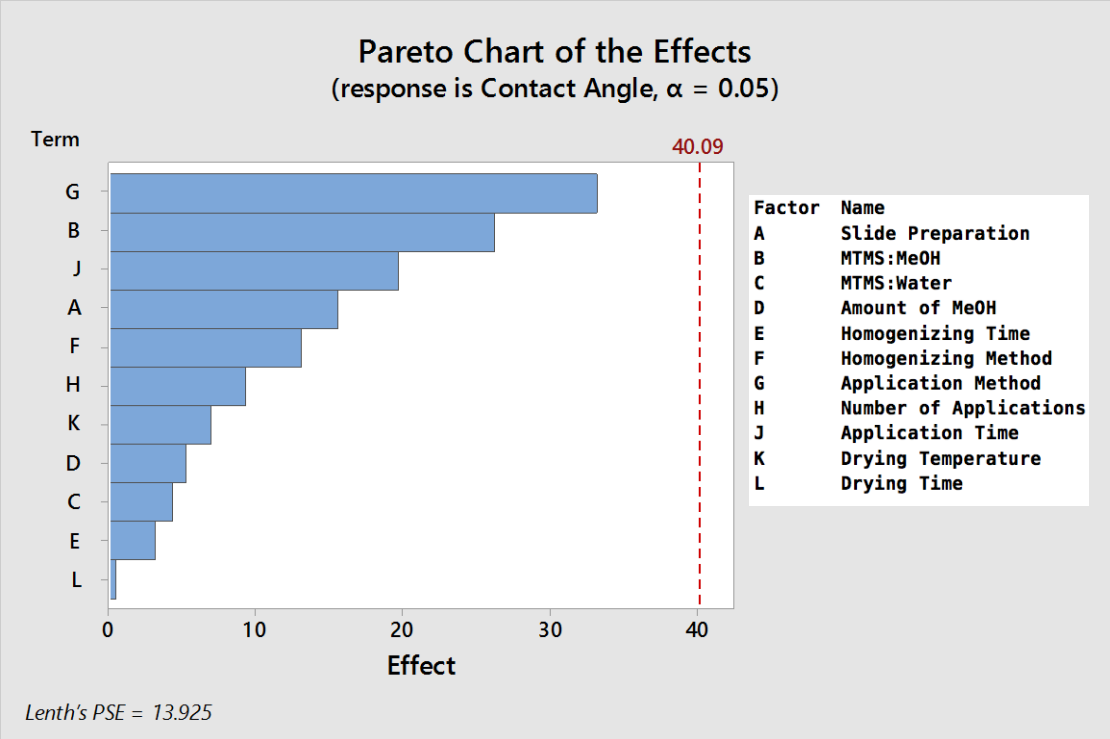


**Figure 21.** Pareto Chart comparing the absolute value of the effects to compare the significance of each value. The effects of each of the factors are not statistically significant within a 95% confidence. The application method and the MTMS to methanol ratio had the greatest effect on the result and the sonication time and drying time had the least amount of an effect.

Though no factor had an effect that was statistically significant within 95% confidence, the relative effect of each factor was compared. The application method had the greatest effect, following by the MTMS to methanol ratio and the application time. The drying time had the smallest effect on the results, followed by the sonication time and the MTMS to water ratio.

This information was used to develop the procedure for making the superhydrophobic surfaces. The sign of the effect of each factor, the relative significance of the effect of each factor and observations made during experimentation were considered when determining what value or technique would be used in the final recipe. The high value of the application method, MTMS:MeOH, slide preparation and homogenizing method was implemented in the final recipe, because these factors all had relatively significant positive effects. The high value of MTMS:Water, 1:8, and the low value of drying time, 150$^{o}$C, were chosen based on the sign of the effect of each these factors but they had relatively less significant effects. Though the effect of the drying

time was positive, it had the least significant effect, so the low value, 1 hour, was chosen for convenience. The homogenization time and amount of methanol used to dissolve the gel also had very little significance and were therefore essentially removed as factors in this procedure. Instead of mixing the gel for a prescribed length of time with a certain amount of methanol, it should be mixed with about 20 mL of methanol until it fully homogenized. The application time and the number of applications were fairly significant. The values for these factors varied most in the literature. Therefore these were further tested with a Multilevel Factorial experimental design, as discussed in the following chapter. Table 9 below summarizes the results.

**Table 9**. Chosen values of each factor for optimized procedure as determined by the results of Plackett-Burman 12-experiment Design.

| Factor | Effect | Chosen Value |
|---|---|---|
| **A** Slide Preparation | 15.650 | Etch |
| **B** MTMS:MeOH | -26.28 | 1:25 |
| **C** MTMS:Water | 4.317 | 1:8 |
| **D** Amount of MeOH | -5.150 | ~20 mL |
| **E** Homogenizing Time | -3.050 | ~5 min |
| **F** Homogenizing Method | 13.150 | Stir bar and stir plate |
| **G** Application Method | 33.25 | Pour |
| **H** Number of Applications | 9.283 | TBD |
| **J** Application Time | -19.683 | TBD |
| **K** Drying Temperature | -6.950 | 150$^{o}$C |
| **L** Drying Time | -0.5167 | 1 hour |

# Chapter 4: Multilevel Factorial Experiment

This chapter details the Multilevel Factorial experimental design used to determine the optimal drying process for the superhydrophobic surfaces. It first discusses the method and application of the experimental design and then provides the results and conclusions. In the following section the coated slides will be referred to as ED-MTMS-*Time-#*, where ED is the experimenters initials, MTMS is the precursor, and *Time-#* refers to the length of time applied and number of applications from the Multifactorial Level design.

## *4.1 Multilevel Factorial Method*

A Multilevel Factorial experimental design is used to create a series of randomized experiments in which all combinations of each level of various factors are tested. The levels are the possible values of each factor. As this is a Multilevel Factorial, each factor may have 2 or more levels. The number of experiments that must be run is based on:

$$X = L_1 * L_2 *.... L_n$$

where X is the total number of experiments that must be run, $L_n$ is the number of levels for the $n_{th}$ factor [32]. For example, if there are 5 factors to test, each with 3 levels, there will be a total 15 experiments.

After completing each experiment a result must be obtained. Using this result, the independent effect of each factor is calculated. Similarly to the Plackett-Burman results, a Pareto chart is used compare the relative effect of each factor and the significance of the effect. Comparing the mean result of each level for each factor compared to the mean result of all experiments shows the main effect of each level [33].

## *4.2 Experimental Design*

From the Plackett-Burman screening process, 2 factors, number of applications and application time, were chosen for further testing. Each factor has three levels that were tested. Table 10 lists the factors and levels used in the Multilevel Factorial experiment.

**Table 10.** List of factors and levels used in the Multilevel Factorial experimental design

| | Factor | |
|---|---|---|
| | **Number of Applications** | **Application Time** |
| Level | 3 | 5 min |
| | 5 | 10 min |
| | 7 | 15 min |

A total of 9 experiments were completed to test all combinations of number of applications and application times. The result for this design is contact angle. Table 11 summarizes the procedure for each of the experiment.

**Table 11.** Precursor molar ratio, dissolving method, slide preparation, application method and drying procedure for each sample based on the Multilevel Factorial experimental design

| | | Sol Dissolving | | | | Application Method | | | Drying | |
|---|---|---|---|---|---|---|---|---|---|---|
| **Sample** | **Molar Ratio (MTMS:MeOH:$H_2O$)** | **Amount of MeOH (mL)** | **Homogenizing Method** | **Time** | **Slide preparation** | **Coating Method** | **Number of Applications** | **Time (min)** | **Temp (ºC)** | **Time (h)** |
| ED-MTMS-5-5 | 1:25:8 | ~20 | Stir | ~5 min | Etched | Pour | 5 | 5 | 150 | 1 |
| ED-MTMS-5-7 | 1:25:8 | ~20 | Stir | ~5 min | Etched | Pour | 7 | 5 | 150 | 1 |
| ED-MTMS-10-3 | 1:25:8 | ~20 | Stir | ~5 min | Etched | Pour | 3 | 10 | 150 | 1 |
| ED-MTMS-10-5 | 1:25:8 | ~20 | Stir | ~5 min | Etched | Pour | 5 | 10 | 150 | 1 |
| ED-MTMS-10-7 | 1:25:8 | ~20 | Stir | ~5 min | Etched | Pour | 7 | 10 | 150 | 1 |
| ED-MTMS-15-3 | 1:25:8 | ~20 | Stir | ~5 min | Etched | Pour | 3 | 15 | 150 | 1 |
| ED-MTMS-15-5 | 1:25:8 | ~20 | Stir | ~5 min | Etched | Pour | 5 | 15 | 150 | 1 |
| ED-MTMS-15-7 | 1:25:8 | ~20 | Stir | ~5 min | Etched | Pour | 7 | 15 | 150 | 1 |

## *4.3 Results and Discussion*

4.3a Qualitative Results

The sol-gels were made as described in *Section 2.1 Aerogel Fabrication Methods.* Most of the sol-gels made in the Multilevel Factorial experiments did not gel like those made in the Plackett-Burman screening process. Not all of the solution gelled in any one of the sol-gels. Some of the gels that did form were clear, while some were white. Furthermore, some of the gels took up to 4 days to gel, compared to 2 days as done previous. Images of the gels are shown in Figure 22.

**Figure 22.** Images of sol-gels used in Multilevel Factorial experiments. Gels did not gel consistently though the same recipe was used. Some gels took up to 4 days to gel and most gels did not fully gel. Some gels were clear and not white.

Due to the difficulty gelling, a gelation study was conducted to determine the possible cause of the problem. The gelation study is described in detail in *Chapter 6: Gelation Study.* Despite the issues, these gels were used to coat the slides according to the process described in *Section 2.1 Aerogel Fabrication Methods.* The slurries made were clumpy and did not appear to pour evenly on the surface of the slide. Most of the slides were coated unevenly. The more applications, the clumpier and flakier the coating appeared to be. The results, including images, key observations, and contact angles, are listed in Table 12. The contact angles did not vary greatly between slides. However, there was a fair amount variation on each slide, as evident by the large standard deviations. This variation in the coating is thought to be due to the gelling issues.

**Table 12.** Key observations, images, average contact angle and highest contact angle image of coated slides from the Multilevel Factorial Experiment. Contact angles are reported as the average with the standard deviation of 10 measurements.

| Experiment | Key Observations | Image | Avg. CA (º) | CA image |
|---|---|---|---|---|
| ED-MTMS-5-3 | Flakey, uneven coating |  | 110.5 ± 11.8 | 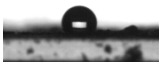 |
| ED-MTMS-5-5 | Flakey, uneven coating. Clumping on edge of slide. |  | 120.7 ± 20.7 | 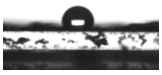 |
| ED-MTMS-5-7 | Flakey, uneven coating |  | 133.1 ± 10.1 | 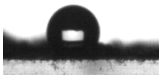 |
| ED-MTMS-10-3 | Flakey, uneven and light coating |  | 112.4 ± 18.2 | 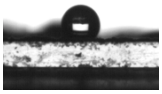 |
| ED-MTMS-10-5 | Flakey, uneven coating |  | 123.8 ± 23.9 |  |
| ED-MTMS-10-7 | Thin light even coating covered by more a flakey uneven coating | 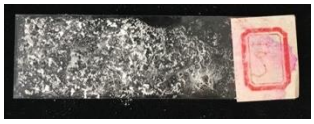 | 130.1 ± 11.1 | 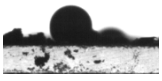 |
| ED-MTMS-15-3 | Thick, flakey, uneven coating. Clumpy with bare spot in middle |  | 121.4 ± 15.0 | 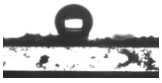 |
| ED-MTMS-15-5 | Thick, flakey, clumpy and uneven coating |  | 116.3 ± 19.1 |  |
| ED-MTMS-15-7 | Thick, flakey, clumpy and uneven coating |  | 133.1 ± 13.8 |  |

## 4.3b SEM Imaging

SEM images were taken of ED-MTMS-10-5 and ED-MTMS-15-5 to look at the coating and compare the structure of the aerogels with different application times. SEM images of ED-MTMS-10-5 are shown in Figure 23.

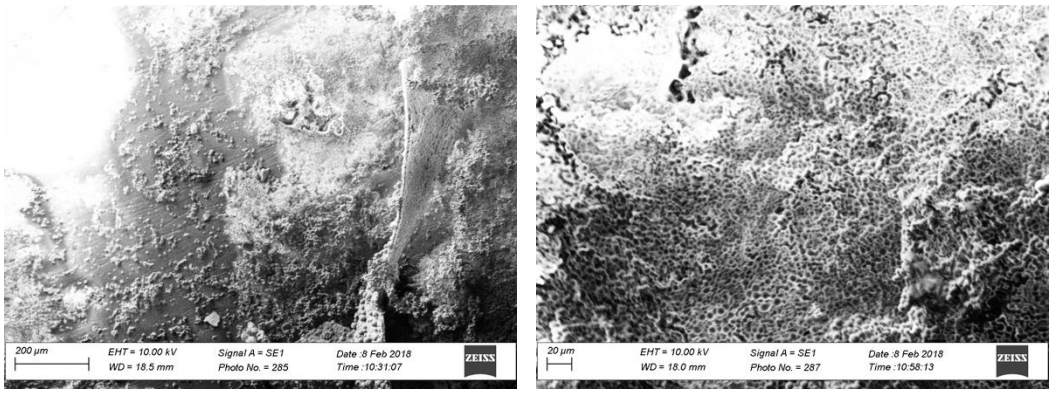


**Figure 23.** SEM images of ED-MTMS-10-5 at a 200 µm (left) and 20 µm (right) scale. Spherical aerogel formation is shown along the surface. The 200 µm scale image shows large gaps between the clumps of aerogel. The etching can be seen on the glass.

The aerogel is in small spherical formations over the surface of the glass. There are large gaps of glass between the aerogel clumps. The etching on the glass can be seen, though it does not appear that aerogel forms in a systematic way along these scratches.

A similar spherical and globular aerogel structure is also seen in the SEM images of ED-MTMS-15-5, as shown in Figure 24.

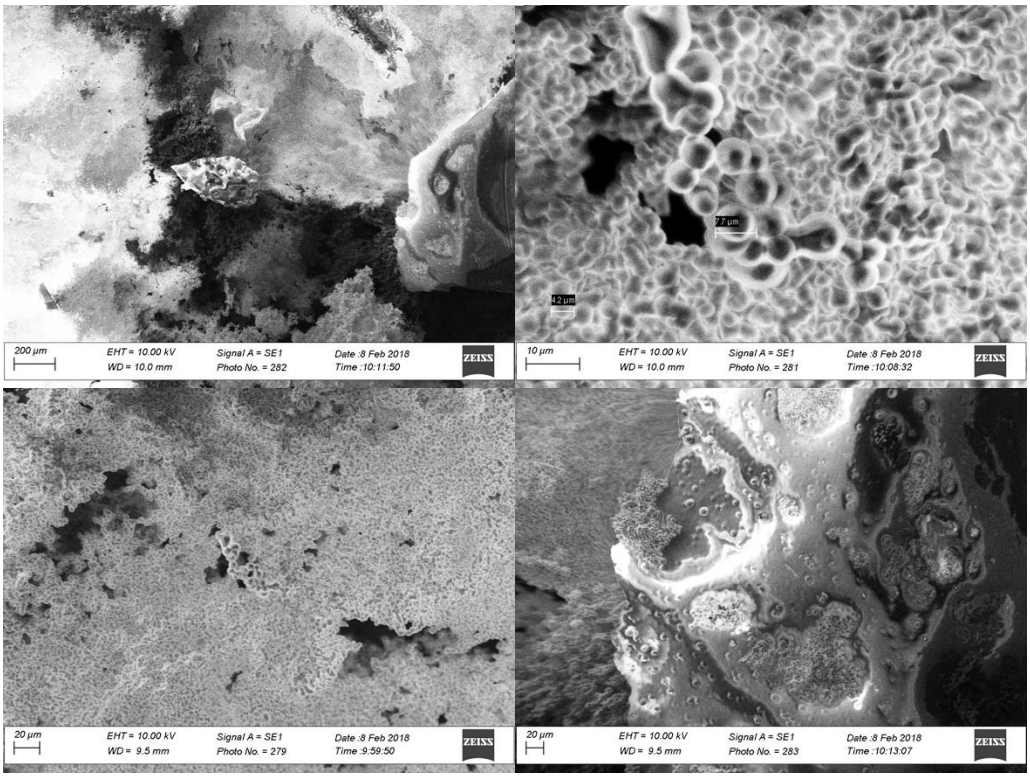


**Figure 24.** SEM images of ED-MTMS-15-5 at a 200 µm (top-left), 10 µm (top-right) and 20 µm (bottom) scale. Spherical and globular aerogel formation is shown along the surface. As shown in the top-right image, the spheres range from about 4 to 7 µm in size.

The size of the spheres range from 4-7 µm, as seen in the top-right image in Figure 24. This formation is also similar, but slightly less uniform, as slide ED-MTMS-08.

## 4.3c Water Testing Results

Water testing was also conducted on ED-MTMS-10-5 and ED-MTMS-15-5. When the slides were run under water, the majority of the aerogel came off of the surface, especially on the ED-MTMS-15-5 slide, as shown by the images in Figure 25.

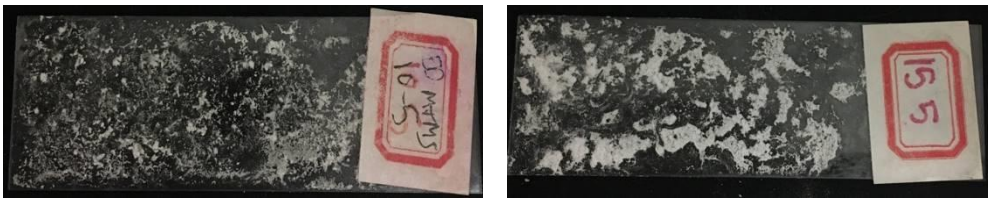

**Figure 25.** Images of ED-MTMS-10-5 and ED-MTMS-15-5 after water testing. A large portion of the aerogel flaked off the surface.

Table 13 lists the contact angle measurements before and after water testing.

**Table 13**. Contact angle measurements before and after water testing

| Slide | Before | After |
|---|---|---|
| ED-MTMS-08 | 123.8 ± 23.9 | 111.4 ± 13.9 |
| ED-MTMS-10 | 116.3 ± 19.1 | 124.3 ± 16.4 |

Despite the major flaking that occurred during water testing, the contact angles did not change, within error.

## 4.3d Multilevel Factorial Results

The contact angle of each experiment was plotted against the number of applications, Figure 26, and by the application time, Figure 27.

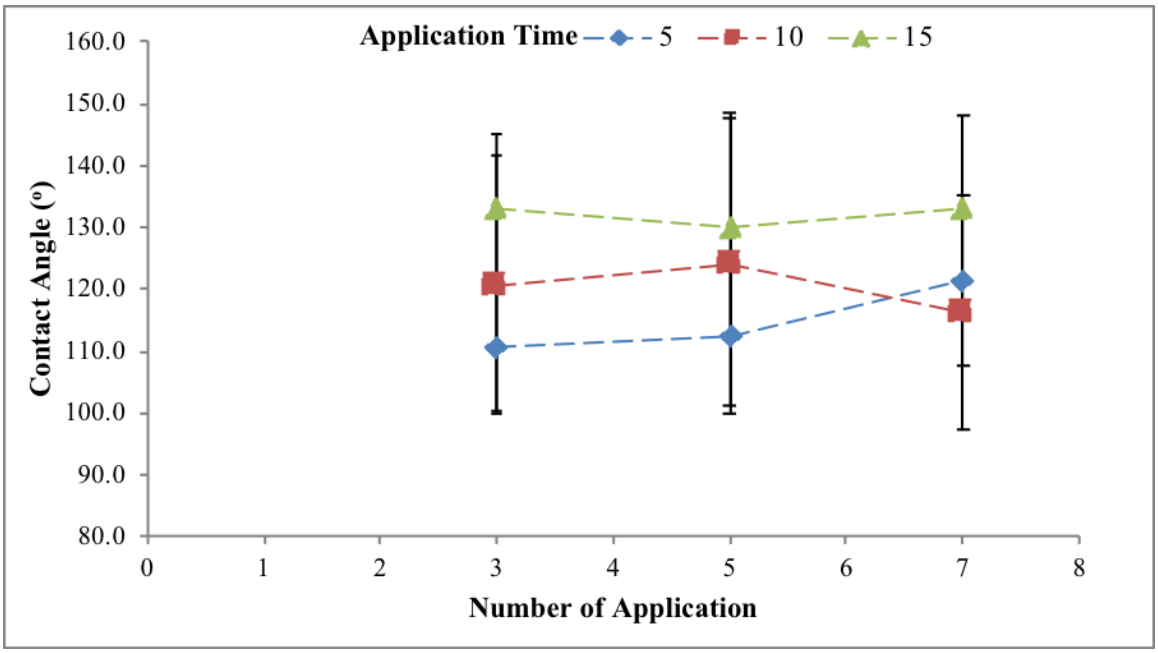


**Figure 26.** Plot of contact angle by number of applications for each application time. The contact angles are fundamentally the same within the standard deviation. The contact angle is greater for all number of applications at 15 minutes application time.

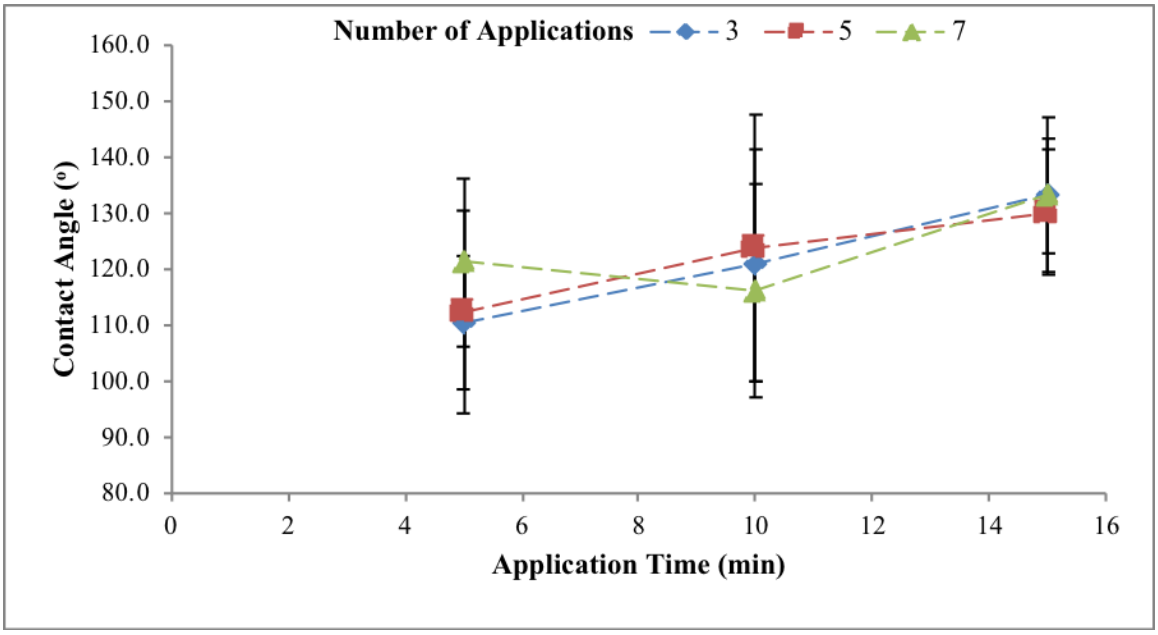


**Figure 27.** Plot of contact angle by application time for each number of applications. The contact angles are fundamentally the same within the standard deviation. The number of applications does not consistently affect the contact angle over the various application times.

These show that, within the standard deviation, the contact angle for each experiment is the same. The plot of contact angle and number of applications for each application time, Figure 26, shows that at 15 minutes the contact angle is consistently greater at any number of applications. The plot of contact angle and application time for each number of applications, Figure 27, shows no consistent pattern between number of applications and contact angle.

Figure 28 shows the Pareto Chart for this experimental design, which charts the absolute value of each effect of each factor.

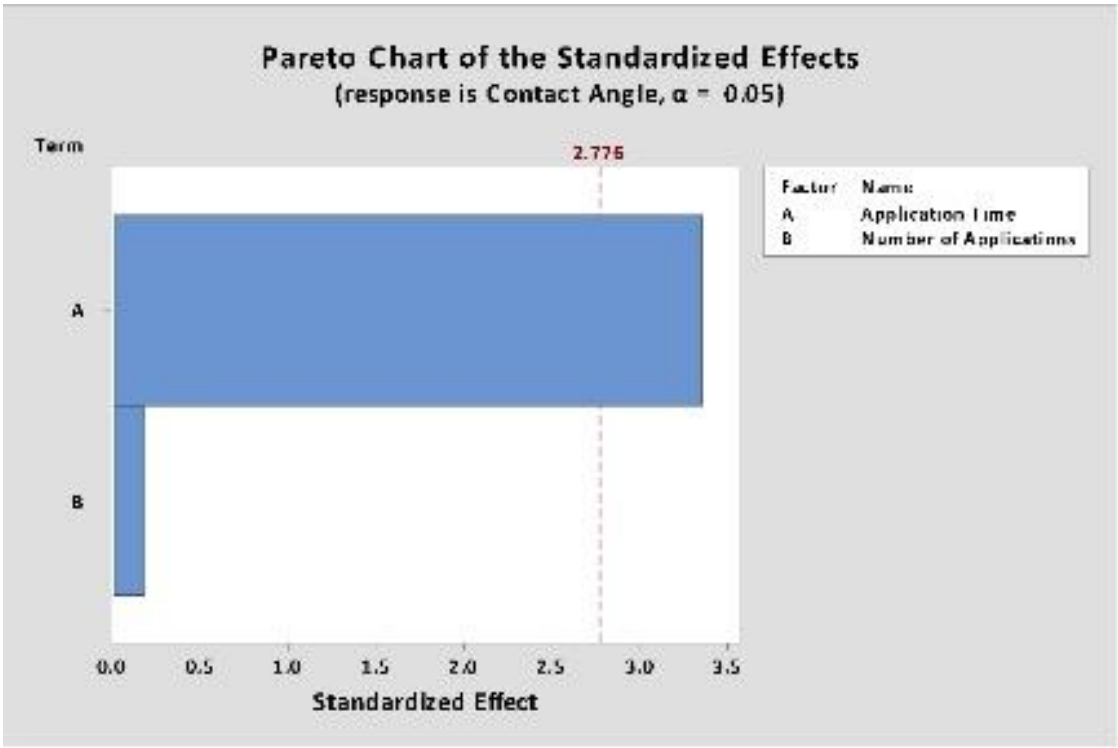


**Figure 28.** Pareto Chart comparing the absolute value of the effects to compare the significance of each value. The effect of the application time is statistically significant within a 95% confidence. The application time has the greatest effect.

This shows that the application time has a statistically significant effect on the result within 95% confidence. The number of applications did not have a statistically significant effect on the result.

A plot of the main effects, in Figure 29, compares the mean result of each level for each factor compared to the mean result of all experiments.

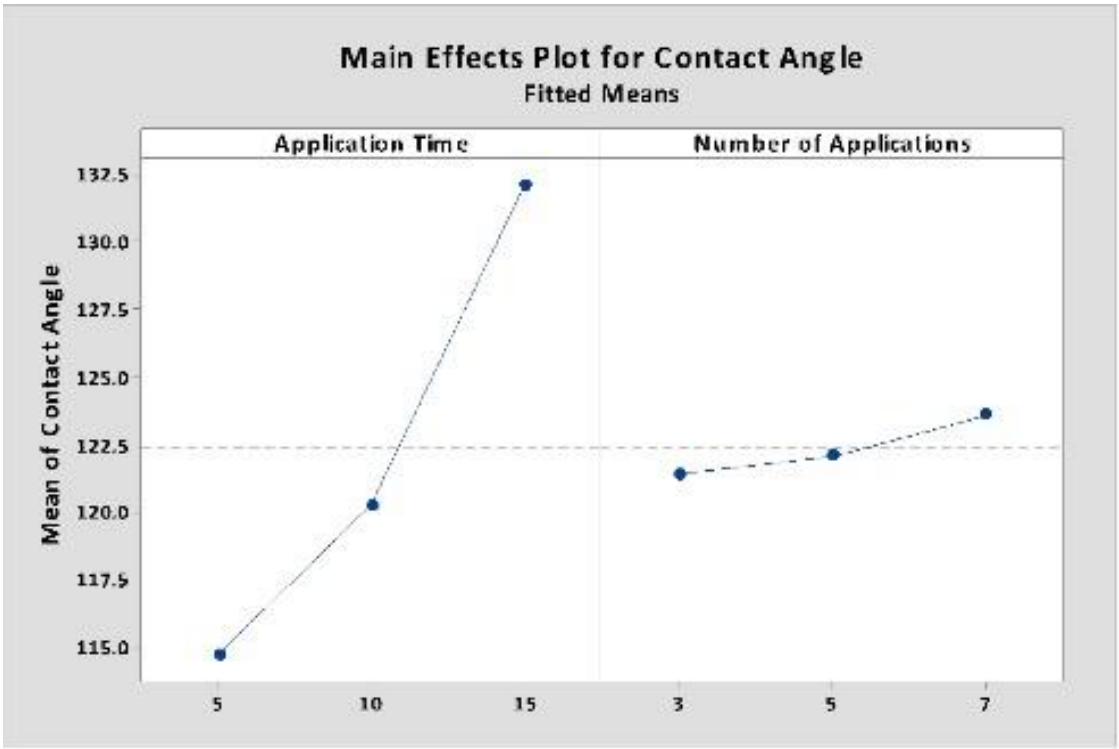


**Figure 29.** Main Effects plot, plotting the mean contact angle of each level factor. The red line denotes the mean contact angle of all experiments. The mean contact angel for each level of application time varies from the mean of all experiments, with an increase in contact angle with 15 minutes time. The mean contact angle of each level of number of applications hardly variesfrom the mean of all experiments.

This plot clearly shows that the application time affects the contact angle because the mean contact angle of for each level varies from the mean of all experiments. With 15 minutes application time, the mean contact angle is greater than the average. Similarly this shows that the number of applications does not change the contact angle significantly.

In conclusion, this experimental design shows that application time has a statistically significant effect on the hydrophobicity of the slide. With 15 minutes application time, there is an increase in the contact angle of the slide, no matter the number of applications. The number of applications does not greatly affect the hydrophobicity of the slide. This agrees with the results from the Plackett-Burman experimental screening, which showed that number of applications had less of an effect on the final result than application time. This information and the information provided by the Plackett-Burman experimental screening is enough to produce a final procedure for making superhydrophobic surfaces.

# Chapter 5: Superhydrophobic Surface Procedure

This chapter goes over the first procedure developed from the experimental designs. The slides produced by the resulting procedure will be referred to as ED-MTMS-R1-## where ED is the experimenters initials, MTMS is the precursor, R1 stands for the first recipe and ## stands for the number slide.

## *5.1 Procedure One*

As discussed in chapters 3 and 4, the results from the Plackett-Burman screening and Multilevel Factorial experiment provide the steps for an optimized procedure. This procedure follows the process described in *Section 2.1Aerogel Fabrication Methods*. The procedure is outline in Table 14.

**Table 14**. Procedure for making superhydrophobic surfaces with silica-based aerogels

| | | |
|---|---|---|
| **Precursor Solution** | **Molar Ratio (MTMS:MeOH:$H_2O$)** | 1:25:8 |
| **Sol Dissolving** | **Amount of MeOH (mL)** | ~20 mL |
| | **Homogenizing Method** | Stir |
| | **Time** | ~5 min |
| **Slide** | **Slide Preparation** | Etch |
| **Application Method** | **Coating Method** | Pour |
| | **Number of Applications** | 3 |
| | **Application Time** | 15 min |
| **Drying Method** | **Temperature** | 150ºC |
| | **Time** | 1 h |

This procedure will be referred to as procedure one or recipe one.

## *5.2 Results and Discussion*

### 5.2a Qualitative Results

A sol-gel was made following the procedure outlined in Table 14. However, the gel was made three times larger so that several slides could be coated from the same sol-gel. The precursor solution was allowed to sit for 72 hours during hydrolysis and 72

hours after condensation to allow for gelling, as opposed to the original 24 hours and 48 hours. This is further discussed in *Chapter 6: Gelation Study*. This is because of the difficulty gelling during the Multilevel Factorial experiments. The solution did not fully gel, as there was some solution left. The sol-gel is shown Figure 29.

**Figure 30.** Image of sol-gel following procedure 1. Some solution sits on top of the white sol-gel.

This gel was used to coat 5 slides with a 15 minute application time. The coatings were very thin and extremely flaky as shown in Table 15, which contains the key observations, images, and contact angles. The decrease in the quality of the coating is thought to be due to the issues during gelation.

**Table 15.** Key observations, images, average contact angle and highest contact angle image of coated slides made following procedure one. Contact angles reported are the average and standard deviation of 10 measurements.

| Experiment | Key Observations | Image | Avg. CA (º) | CA image |
|---|---|---|---|---|
| ED-MTMS-R1-01 | Light, uneven, dusty coating | 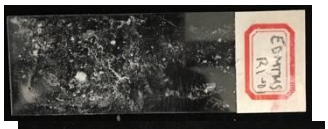 | 121.6 ± 17.5 | 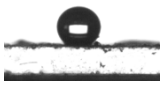 |
| ED-MTMS-R1-02 | Flakey, uneven coating | 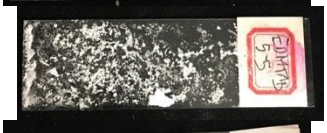 | 118.0 ± 16.1 | 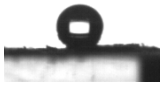 |
| ED-MTMS-R1-03 | Flakey, uneven coating and light dusty coating | 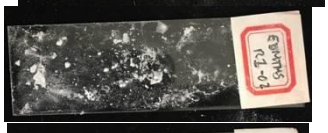 | 110.5 ± 15.7 | 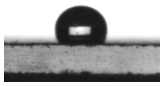 |
| ED-MTMS-R1-04 | Flakey, uneven and light coating |  | 126.6 ± 8. 6 | 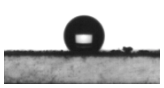 |
| ED-MTMS-R1-05 | Flakey, uneven coating |  | 112.2 ± 13.0 | 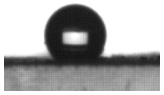 |

5.2b SEM Imaging

The surface of ED-MTMS-R1-01 was imaged using the SEM. As shown in Figure 31, the same 4-7 μm sized spherical aerogel formation is seen along the surface.

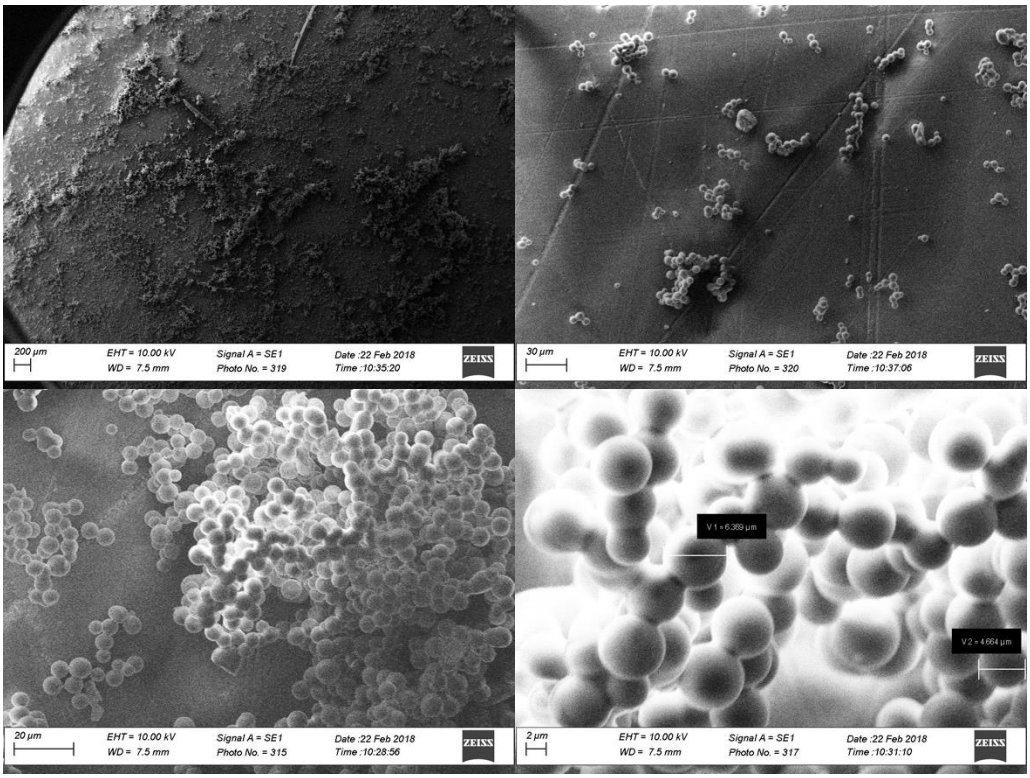


**Figure 31.** SEM images of ED-MTMS-R1-01 at a 200 μm (top-left), 30 μm (top-right), 20 μm (bottom-left) and 2 μm scale. Spherical aerogels of 4-7 μm are formed a long the surface, as shown in the bottom right image. The top two images show that there are large spaces between the aerogel clumps. Etching on the glass slide is seen.

The surface is coated very unevenly, as large gaps with no aerogel are clearly seen in the top two images in Figure 31. Again, the etching on the slide is seen but the aerogel does not seem to form to these etchings.

Theses images show that aerogel on these slides are similar to ED-MTMS-08, ED-MTMS-10-5 and ED-MTMS-15-5, despite the gelation issues. However, the decrease in durability and evenness of the coatings suggests the gelation issues could have an effect on the quality. Therefore a gelation study, as detailed in the following chapter, was conducted.

# Chapter 6: Gelation Study

As discussed in *Section 4.3 Multilevel Factorial Results and Discussion,* issues with gelation began to occur during the Multilevel Factorial experiment. The gels did not fully gel and were clear, unlike the gels made previously during the Plackett-Burman screening. These issues with gelling persisted throughout the rest of the study. The slides that were coated with the unsatisfactory gels in the Multilevel Factorial experiment and in testing procedure one were uneven and flakey. This is likely due to the issues with the sol-gel. Therefore the rest of the study was focused on determining the source of the gelation problem. This chapter will first discuss some of the alterations made in an effort to improve the sol-gels. It will then discuss an alternative recipe that was attempted and its results. Finally it will discuss the quality of the MTMS and its possible effects on gelation.

## *6.1 Alterations to the Recipe and Results*

To improve the quality of the sol-gels and pin-point the source of error in the failed gels seven different attempts were made: (1) adjusting the condensation time, (2) adjusting the hydrolysis time, (3) remaking the catalyst, (4) remaking the oxalic acid, (5) decreasing batch size, (6) varying the MTMS:MeOH:$H_2O$ and (7) adjusting the mixing with various MTMS:MeOH:$H_2O$. Each of these is discussed below.

(1) Condensation Time: The length of time for condensation was extended to up to 4 days for the Multilevel Factorial experimental sol-gels. These gels did not fully gel, as shown in the previous chapter in Figure 22.

(2) Hydrolysis Time: The hydrolysis time was lengthened to see if there was an issue at this step of the process. Two sol-gels were made during this attempt, one that sat for two days and one that sat for three days before adding the ammonium hydroxide catalyst. These sol-gels were three times the size of the sol-gels originally made in the Plackett-Burman screening so that several slides could be coated from one gel to test Procedure 1. The gel that sat for two days did not gel.

The one that sat for three days gelled some but not fully. The latter was still used in testing Procedure 1. Images of the two gels are shown in Figure 32 below.

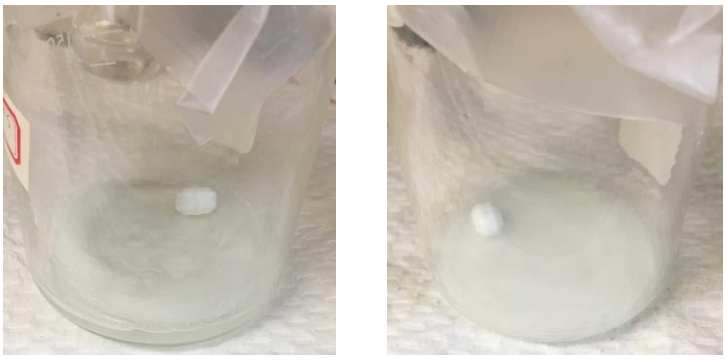

**Figure 32.** Image of two triple-batch gels made to test the hydrolysis time. The left gel was given 2 days for hydrolysis and did not gel. The right gel was given 3 days for hydrolysis and some gelling occurred. This is the gel used in Procedure One.

(3) Catalyst: The next gel was an attempt to repeat the triple batch size sol-gel made with 3 days of hydrolysis but with ammonium hydroxide catalyst that was re-made fresh. However the solution dried out and formed a hard film before the catalyst was added, as shown in Figure 33.

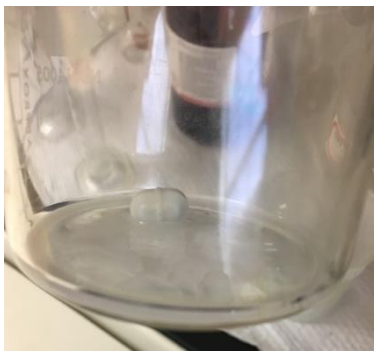

**Figure 33.** Image of triple-batch precursor solution that hardened after three days before addition of the ammonium hydroxide catalyst.

(4) Oxalic acid: This sol-gel was made as a triple batch, allowing only 1 day for hydrolysis, using the freshly made oxalic acid and catalyst. Again, the solution did not gel. Rather a film, similar to the one in the previous attempt, formed but in the solution, as shown in Figure 34.

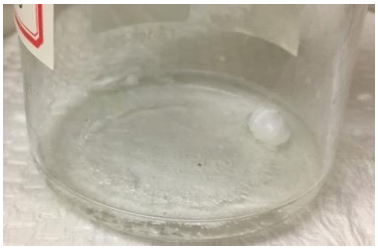

**Figure 34.** Image of triple-batch gel made with fresh oxalic acid and ammonium hydroxide. A film formed at the bottom in a solution.

(5) Decrease Batch Size: Three gels were made at the original batch size, to see if the increasing batch size affected the quality of the gel. These were given 1 day for hydrolysis and used the same oxalic acid and ammonium hydroxide as the previous attempt. Again, as seen in Figure 35, a film formed in the solution.

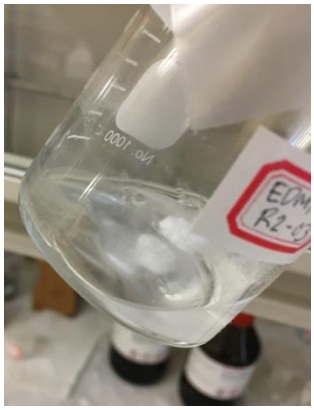

**Figure 35.** Image of one of the three gels made at the original batch size. The solution did not gel but a clear film was formed at the bottom in a solution.

(6) Vary MTMS:MeOH:$H_2O$: Up to this point, all the gels made had the same molar ratio of MTMS:MeOH:$H_2O$ of 1:25:8. To determine whether the amount of each reagent in the precursor solution was now affecting the gel, four gels with different ratios were made. The ratios were based on the original ratios tested in the Plackett-Burman Screening Process, 1:25:0, 1:25:8, 1:35:0, 1:35:8. The 1:25:0 formed a gel but did not gel fully. The other three formed the film seen in previous attempts. Figure 36 displays the images of these for gels.


**Figure 36.** Image of the gels made with an MTMS:MeOH:$H_2O$ ratio of (from left to right) 1:25:0, 1:25:8, 1:35:0, 1:35:8. The 1:25:8 appeared to partially gel, while the other three formed the clear film in solution.

(7) Stirring: This attempt also varied the MTMS:MeOH:$H_2O$ but the solution was stirred for the entire 24 hours given for hydrolysis. This was done to assure that the solution was homogenous. Again, films and no gels were formed, as seen in Figure 37.

**Figure 37.** Image of the gels made with an MTMS:MeOH:$H_2O$ ratio of (from left to right) 1:25:0, 1:25:8, 1:35:0, 1:35:8.

## *6.2 Alternative Recipe*

Due to the lack of success in the attempts discussed in *Section 5.1 Alterations and Results*, a new recipe was tested. This recipe is used by Union College to produce superhydrophobic aerogels with the RSCE method. This recipe forms sol-gels within a few hours. The recipe uses both tetramethylorthosilicate, TMOS, and MTMS in varying percentage amounts. Typically these gels are not dried at ambient temperature, but in order to find out why the gels were not forming this method was attempted. The recipes for these aerogels, with the various MTMS percentages are given shown in Table 16.

**Table 16.** Recipe for TMOS/MTMS wet-gels with various percentages of MTMS

| Chemical | 75 % | 50% | 25 % |
|---|---|---|---|
| TMOS (mL) | 1.06 | 2.125 | 3.19 |
| MTMS (mL) | 3.19 | 2.125 | 1.06 |
| MeOH (mL) | 13.75 | 13.75 | 13.75 |
| $H_2O$ (mL) | 1.80 | 1.80 | 1.80 |
| 1.5 M $NH_4OH$ (mL) | 0.134 | 0.134 | 0.134 |

The 50% and 25% MTMS solutions gelled with a few hours. The gels were transparent and had a slight blue tint to them, as shown in Figure 38.

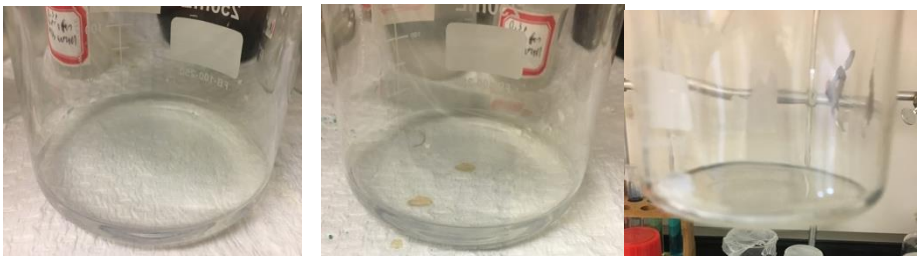

**Figure 38.** Image of (from left to right) 25%, 50% and 75% sol-gels. The 25% and 50% gels fully gelled and are clear with a blue tint. The 75% solution did not gel and appears to have evaporated.

The 75% solution however did not gel, also shown in Figure 36. After 24 hours the solution volume decreased, suggesting that the solution may have evaporated. Since the solutions with less MTMS were able to gel, it is possible that the gelation issues are due to the MTMS.

The 25% and 50% MTMS gels were then dissolved in 20 mL of methanol. The solutions were dissolvable and formed fairly homogenous slurries, as shown in Figure 39.

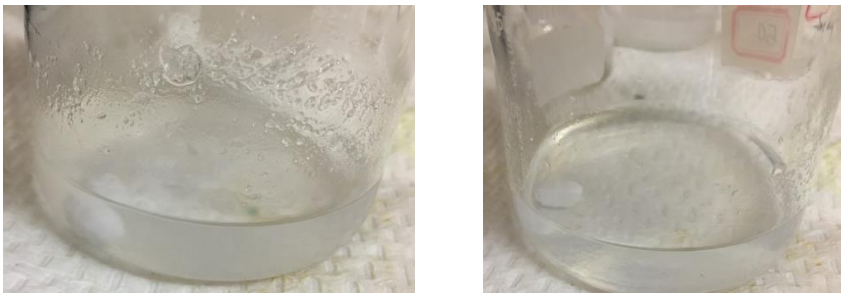

**Figure 39.** Image of 25% and 50% MTMS gels dissolved in methanol. The gels dissolved to form a fairly homogenous slurry.

These were coated onto the slides following the procedure used in the Plackett-Burman screening for the ED-MTMS-08 because this slide had the highest average contact angle and the most even, uniform coating. The slides coated with the RSCE recipe aerogels will be referred to as ED-TMOS%%MTMS where %% is the percent MTMS in the precursor solution. Both coating on both slides was very light and uneven. The layers of aerogel flaked off the slide when moved in and out of the drying furnace. Images of the slides, as well as key observations and contact angles are listed in Table 17.

**Table 17.** Key observations, images, average contact angle and highest contact angle image of coated slides made with RSCE aerogel recipe

| Experiment | Key Observations | Image | Avg. CA (º) | CA image |
|---|---|---|---|---|
| ED-TMOS25MTMS | Extremely light coating |  | 76.3 ± 12.5 | 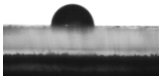 |
| ED-TMOS50MTMS | Flakey, uneven and light coating | | 93.0 ± 13.5 |  |

## *6.3 MTMS Study*

None of the various attempts discussed in *Section 6.1 Alterations and Results* resulted in gels that were similar to those originally made during the Plackett-Burman screening. The solutions made according the RSCE recipe gelled when 25% and 50% MTMS was used but not when 75% MTMS was used. This could mean that the MTMS is affecting the gel. All of the MTMS was bought in 2013 or 2015. Therefore it is possible that it has degraded in that time. In order to determine whether this is the case, the density of the MTMS from each bottle was calculated and compared to the actual density, 0.955 g/mL [34]. The mass of 1 mL of MTMS was measured on an analytic balance. Only one measurement was made, so this should be repeated for a more statistically significant measurement. The densities in g/mL of four bottles are listed in Table 18.

**Table 18.** Density of Various MTMS

| Bottle Number | Date Bought | Density (g/mL) |
|---|---|---|
| 1 | 5/21/15 | 0.9042 |
| 2 | 5/21/15 | 0.9032 |
| 3 | 4/24/13 | 0.9307 |
| 4 | 4/24/13 | 0.9014 |

Note that bottles 1 and 4 were used for the gels made throughout this study. The MTMS in all the bottles, except bottle 3, have densities about 5% to 6% lower than the reported density of MTMS. This suggests that MTMS may be degraded and could cause some error during gelation.

# Chapter 7: Summary and Future Work

## *7.1 Summary*

The initial Plackett-Burman Screening experiments show that it is possible to coat the glass slides and receive hydrophobic coatings. Slide ED-MTMS-08 had an average contact angle of 132.8 ± 7.8 and was evenly coated. Water testing showed that it could with stand exposure to water. SEM imaging revealed a spherical microstructure formed by the aerogel on the surface. These structures are similar to those discovered in Rao et al. [28] study. Additionally, this structure vaguely resembles the papilla structure of the lotus leaf [4]. Thus it is likely that these structures contribute the hydrophobicity of the slides. The Plackett-Burman screening also determined which factors had the most relative significance on the hydrophobicity of the slide. The application method and MTMS:MeOH ratio had the greatest relative effect on the quality of the surface, while drying time and homogenizing time had very little effect. Further experimental testing, conducted under a Multilevel Factorial design, showed that increasing the application time to 15 minutes had a positive effect on the hydrophobicity of the slide. It also suggested that the number of applications does not greatly affect the quality of the slide. The coated slides in this experimental design also had the spherical microstructure. Nevertheless a maximum contact angle of 156$^{o}$ was achieved on slide ED-MTMS-10-5. A procedure was outlined and tested from the results of the two experimental designs.

Though the procedure was tested, issues regarding gelation occurred. The slides that were produced after the Plackett-Burman screening process were lower quality. This is likely due to these gelation issues. Several alterations were made to the procedure to try and determine the source of the problem. Adjustments to the hydrolysis time, condensation time, the reagents, the size of the precursor solution and more were made, yet gelation was not improved. Gels made using the RSCE recipe suggest that the MTMS may be the root of the problem. The precursor solutions made with 25% and 50% MTMS gelled, while the 75% MTMS solution did not. Furthermore, the densities of the MTMS vary from the density of MTMS, suggesting that the MTMS had degraded. One study by Dong et al. [35] looked at the effects of pH on MTMS gelation. The study used different concentrations and combinations of HCl and $NH_4OH$ as the catalyst. The study found that

at a pH of 4-5 or greater than 11 produced monolithic gels, while at a pH less than 3 or between 5-8, a resin in solution was formed. This resin looks similar to the film observed in this study. Thus pH may also play a possible role in the gelation problem. The first step in continuing this project will be to pin-point the gelation issue.

## *7.2 Future Work*

Future work for this project will include: a) identify gelation issues, b) producing a repeatable procedure for superhydrophobic surface production and c) testing drag.

(a) Gelation Issues: Before moving forward with this project, the problems occurring during gelation must be addressed. The first suggestion for would be to purchase fresh MTMS and repeat the procedure carried out for slide ED-MTMS-08. Since this slide was coated well, similar results should be produced if the gel is made correctly. If this does not solve the problem, the next suggestion would be to look into varying the pH of the solution. Based on a study by Dong et al. [35], the pH level has an effect on the gelation quality when using MTMS. Another suggestion would be to look at the temperature during condensation and hydrolysis. It is possible that the temperature could have a significant enough effect on the gelation. Therefore varying the temperature may address the problem. Once the gelation issue is resolved, the procedure will be robust and repeatable.

(b) Repeatable Procedure: Several slides should be produced using procedure one and characterized using contact angle measurements and SEM imaging. It may also be advantageous to repeat the Multilevel Factorial design to assure that the same or similar results are obtained with better quality gels. Adjustments and further testing of the procedure should be completed until the surfaces are superhydrophobic and evenly coated.

(c) Drag Tests: When satisfactory slides are produced they should be tested using micro-Particle image velocimetry. This is a method used to image fluid flows over surfaces and produce a velocity profile. The slides should also be tested for drag with a rotational viscometer. This measures the force exerted on a rotating spindle. In order to do this, the procedure must be adapted to coat the

spindle instead of the glass slide. One suggestion is to manufacture a glass plate that can attach to the end of the spindle and that will be easily coated.

Other areas to investigate relating to this project could look at using RSCE aerogels, coating surfaces other than glass slides or using an adhesive to coat the aerogel. These were ideas that were initially contemplated but not actualized due to time constraints and focus of the project.

## References


[1] Li, X. M., Reinhoudt, D., and Crego-Calama, M., 2007, "What do we need for a superhydrophobic surface? A review on the recent progress in the preparation of superhydrophobic surfaces," Chemical Society Reviews, **36**(8), pp. 1350-1368.

[2] "Contact Angle," from https://en.wikipedia.org/wiki/Contact_angle

[3] Shibuichi, S., Onda, T., Satoh, N., and Tsujii, K., 1996, "Super water-repellent surfaces resulting from fractal structure." The Journal of Physical Chemistry, **100**(50), pp. 19512-19517.

[4] Sun, T., Feng, L., Gao, X., and Jiang, L., 2005, "Bioinspired surfaces with special wettability." Accounts of chemical research, **38**(8), 644-652.

[5] Heimbuch, J., "NASA Uses Lotus Leaf As Inspiration for Space Gear Dust-Repellent," from https://www.treehugger.com/clean-technology/nasa-uses-lotus-leaf-as-inspiration-for-space-gear-dust-repellent.html.

[6] Barthlott, W., and Neinhuis, C., 1997, "Purity of the sacred lotus, or escape from contamination in biological surfaces," Planta, **202**(1), pp. 1-8.

[7] Li, Y., Cai, W., Duan, G., Cao, B., Sun, F., and Lu, F., 2005, "Superhydrophobicity of 2D ZnO ordered pore arrays formed by solution-dipping template method," Journal of colloid and interface science, **287**(2), pp. 634-639.

[8] Pozzato, A., Dal Zilio, S., Fois, G., Vendramin, D., Mistura, G., Belotti, M., and Natali, M., 2006, "Superhydrophobic surfaces fabricated by nanoimprint lithography," Microelectronic Engineering, **83**(4-9), pp. 884-888.

[9] Balu, B., Breedveld, V., and Hess, D. W., 2008, "Fabrication of "roll-off" and "sticky" superhydrophobic cellulose surfaces via plasma processing," Langmuir, **24**(9), pp. 4785-4790.

[10] Zhang, G., Wang, D., Gu, Z. Z., and Möhwald, H., 2005, "Fabrication of superhydrophobic surfaces from binary colloidal assembly," Langmuir, **21**(20), pp. 9143-9148.

[11] Li, Y., Liu, F., and Sun, J., 2009, "A facile layer-by-layer deposition process for the fabrication of highly transparent superhydrophobic coatings," Chemical communications, (19), pp. 2730-2732.

[12] Ma, M., Mao, Y., Gupta, M., Gleason, K. K., and Rutledge, G. C., 2005, "Superhydrophobic fabrics produced by electrospinning and chemical vapor deposition," Macromolecules, **38**(23), pp. 9742-9748.

[13] Khayet, M., Mengual, J. I., and Matsuura, T., 2005, "Porous hydrophobic/hydrophilic composite membranes: application in desalination using direct contact membrane distillation," Journal of Membrane Science, **252**(1-2), pp. 101-113.

[14] Ou, J., Perot, B., and Rothstein, J. P., 2004, "Laminar drag reduction in microchannels using ultrahydrophobic surfaces," Physics of fluids, **16**(12), pp. 4635-4643.

[15] Lee, C., Choi, C.H., and Kim, C.J., 2016, "Superhydrophobic drag reduction in laminar flows: a critical review," Experimental Fluids, **57**(12), pp. 176.

[16] Daniello, R. J., Waterhouse, N. E., and Rothstein, J. P., 2009, "Drag reduction in turbulent flows over superhydrophobic surfaces," Physics of Fluids, **21**(8), pp. 085103.

[17] Maali, A., and Bhushan, B., 2012, "Measurement of slip length on superhydrophobic surfaces," Phil. Trans. R. Soc. A, **370**(1967), pp. 2304-2320.

[18] Ou, J., and Rothstein, J. P., 2005, "Direct velocity measurements of the flow past drag-reducing ultrahydrophobic surfaces," Physics of Fluids, **17**(10), 103606.

[19] Truesdell, R., Mammoli, A., Vorobieff, P., van Swol, F., and Brinker, C. J., 2006, "Drag reduction on a patterned superhydrophobic surface," Physical review letters, **97**(4), pp. 044504.

[20] Aegerter, M.A., Leventis, N., and Koebel, M.M., Eds., 2011, *Aerogels Handbook*, Springer Science+Business Media, New York, NY, Chap. 3-4.

[21] "About Aerogels." from https://muse.union.edu/aerogels/sample-page/

[22] Hrubesh, L. W., and Poco, J. F., 1995, "Thin aerogel films for optical, thermal, acoustic and electronic applications," Journal of non-crystalline solids, **188**(1-2), pp. 46-53.

[23] Bhagat, S. D., Oh, C. S., Kim, Y. H., Ahn, Y. S., and Yeo, J. G., 2007, "Methyltrimethoxysilane based monolithic silica aerogels via ambient pressure drying," Microporous and mesoporous Materials, **100**(1), pp. 350-355.

[24] Budunoglu, H., Yildirim, A., Guler, M. O., and Bayindir, M., 2011, “Highly transparent, flexible, and thermally stable superhydrophobic ORMOSIL aerogel thin films,” ACS applied materials & interfaces, **3**(2), pp. 539-545.

[25] Kim, A., Kim, H., Lee, C., and Kim, J., 2014, “Effective three-dimensional superhydrophobic aerogel-coated channel for high efficiency water-droplet transport,” Applied Physics Letters, **104**(8).

[26] Kim, A., Kim, H., and Kim, J., 2013, “Effective three-dimensional superhydrophobic channel coating using organically modified silica aerogel,” Micro Electro Mechanical Systems (MEMS), pp. 1207-1210.

[27] Fei, T., Chen, H., and Lin, J., 2014, “Transparent superhydrophobic films possessing high thermal stability and improved moisture resistance from the deposition of MTMS-based aerogels,” Colloids and Surfaces A: Physicochemical and Engineering Aspects, **443**, pp. 255-264.

[28] Rao, A.V., Manish, M.K., Bhagat, S.D., 2005, “Transport of liquids using superhydrophobic aerogels,” Journal of Colloid and Interface Science, **285**, pp. 413-418.

[29] Gauthier, B.M., Bakrania, S.D., Anderson, A.M., and Carroll, M.K., 2004, "A fast supercritical extraction technique for aerogel fabrication," Journal of non-crystalline solids, **350**, 238-243.

[30] Barabasz, R., 2011, “Effects of Superhydrophobic Aerogel Surface Coatings on Drag Reduction,” Senior Project Report, Union College Department of Mechanical Engineering, Schenectady, NY.

[31] Rodriguez, J. E., Anderson, A. M., and Carroll, M. K., 2014, “Hydrophobicity and drag reduction properties of surfaces coated with silica aerogels and xerogels,” Journal of sol-gel science and technology, **71**(3), pp. 490-500.

[32] Analytical Methods Committee, 2013, “Experimental design and optimization (4): Plackett-Burman designs,” Analytical Methods, **5**(8), pp. 1901-1903.

[33] “Designing an Experiment.” from https://support.minitab.com/en-us/minitab/18/getting-started/designing-an-experiment/#create-a-designed-experiment.

[34] “Trimethoxymethylsilane.” from https://support.minitab.com/en-us/minitab/18/getting-started/designing-an-experiment/#create-a-designed-experiment.

[35] Dong, H., Brook, M. A., and Brennan, J. D., 2005, “A new route to monolithic methylsilsesquioxanes: gelation behavior of methyltrimethoxysilane and morphology of resulting methylsilsesquioxanes under one-step and two-step processing,” Chemistry of materials, **17**(11), pp. 2807-2816.

## Acknowledgements

The author would like to acknowledge and thank the Union College Aerogel Lab Advisors, Professors Ann Anderson, Mary Carroll and Bradford Bruno, as well as the other members of the aerogel lab. The author would like to acknowledge MJ Lee for her contributions to contact angle measurements and Craig Scharf (Math ’18) for his assistance with the Plackett-Burman experimental design set up. This project would not have been possible without funding for the Aerogel Lab through the NSF RUI LHE – 0847901 and NSF MRI CMMI-0722842 and funding through Union College Student Research Grants.

## Appendices

*Appendix A – Contact Angle Measurements*

# Appendix A – Contact Angle Measurements

**Table A.1** Contact angle measurements from slides from Plackett-Burman screening.
(Note: cells highlighted in red had a drop size of 4 μL. Those highlighted in pink had a drop size of 3 μL. Cells highlighted in blue were taken after water testing.)

| Experiment # | FILE NAME | CA Left | CA Right | Average | Std Dev |
|---|---|---|---|---|---|
| 1.0 | EDMTMS01_01 | 87.6 | 87.9 | 87.8 | |
| 1.0 | EDMTMS01_02 | 82.6 | 83.3 | 83.0 | |
| 1.0 | EDMTMS01_03 | 83.1 | 82.4 | 82.8 | |
| 1.0 | EDMTMS01_04 | 90.9 | 91.1 | 91.0 | |
| 1.0 | EDMTMS01_05 | 90.1 | 88.3 | 89.2 | |
| 1.0 | EDMTMS01_06 | 93.1 | 92.6 | 92.9 | |
| 1.0 | EDMTMS01_07 | 96.0 | 96.1 | 96.1 | |
| 1.0 | EDMTMS01_08 | 90.6 | 96.8 | 93.7 | |
| 1.0 | EDMTMS01_09 | 95.4 | 95.8 | 95.6 | 4.6 |
| 1.0 | EDMTMS01_10 | 93.3 | 93.3 | 93.3 | 5.2 |
| **1.0** | **AVERAGE** | **90.3** | **90.8** | **90.5** | **4.8** |
| 2.0 | NA | 89.7 | 88.8 | 89.3 | |
| 2.0 | NA | 117.2 | 115.2 | 116.2 | |
| 2.0 | EDMTMS2_01 | 120.4 | 122.2 | 121.3 | |
| 2.0 | EDMTMS2_02 | 104.6 | 104.8 | 104.7 | |
| 2.0 | EDMTMS2_03 | 91.0 | 84.1 | 87.6 | |
| 2.0 | EDMTMS2_04 | 92.5 | 94.4 | 93.5 | |
| 2.0 | EDMTMS2_05 | 113.6 | 114.1 | 113.9 | |
| 2.0 | EDMTMS2_06 | 120.0 | 117.6 | 118.8 | |
| 2.0 | EDMTMS2_07 | 106.5 | 106.9 | 106.7 | |
| 2.0 | EDMTMS2_08 | 126.3 | 126.4 | 126.4 | |
| 2.0 | EDMTMS2_09 | 103.9 | 104.7 | 104.3 | 12.5 |
| 2.0 | EDMTMS2_10 | 98.8 | 95.9 | 97.4 | 13.4 |
| **2.0** | **AVERAGE** | **107.0** | **106.3** | **106.7** | 12.9 |
| 3.0 | EDMTMS3_01 | 113.5 | 113.1 | 113.3 | |
| 3.0 | EDMTMS3_02 | 102.4 | 105.2 | 103.8 | |
| 3.0 | EDMTMS3_03 | 101.6 | 99.9 | 100.8 | |
| 3.0 | EDMTMS3_04 | 122.4 | 118.0 | 120.2 | |
| 3.0 | EDMTMS3_05 | 128.4 | 128.2 | 128.3 | |
| 3.0 | EDMTMS3_06 | 132.7 | 133.1 | 132.9 | |
| 3.0 | EDMTMS3_07 | 131.6 | 132.6 | 132.1 | |
| 3.0 | EDMTMS3_08 | 137.6 | 137.3 | 137.5 | |
| 3.0 | EDMTMS3_09 | 123.1 | 122.5 | 122.8 | 12.7 |
| 3.0 | EDMTMS3_10 | 130.8 | 130.8 | 130.8 | 12.7 |
| **3.0** | **AVERAGE** | **122.4** | **122.1** | **122.2** | 12.6 |

| | | | | | |
|---|---|---|---|---|---|
| 4.0 | EDMTMS04_01 | 15.0 | 15.0 | 15.0 | |
| 4.0 | EDMTMS04_02 | 46.4 | 53.6 | 50.0 | |
| 4.0 | EDMTMS04_03 | 42.6 | 39.5 | 41.1 | |
| 4.0 | EDMTMS04_04 | 51.0 | 52.4 | 51.7 | |
| 4.0 | EDMTMS04_05 | 50.6 | 38.5 | 44.6 | |
| 4.0 | EDMTMS04_06 | 47.8 | 49.0 | 48.4 | |
| 4.0 | EDMTMS04_07 | 36.8 | 39.2 | 38.0 | |
| 4.0 | EDMTMS04_08 | 44.7 | 46.9 | 45.8 | |
| 4.0 | EDMTMS04_09 | 39.0 | 40.4 | 39.7 | 10.6 |
| 4.0 | EDMTMS04_10 | 36.2 | 39.3 | 37.8 | 10.9 |
| **4.0** | **AVERAGE** | **41.0** | **41.4** | **41.2** | **10.4** |
| 5.0 | EDMTMS5_01 | 91.7 | 91.5 | 91.6 | |
| 5.0 | EDMTMS5_02 | 88.6 | 87.1 | 87.9 | |
| 5.0 | EDMTMS5_03 | 85.6 | 85.3 | 85.5 | |
| 5.0 | EDMTMS5_04 | 90.0 | 90.0 | 90.0 | |
| 5.0 | EDMTMS5_05 | 90.4 | 91.5 | 91.0 | |
| 5.0 | EDMTMS5_06 | 82.6 | 85.3 | 84.0 | |
| 5.0 | EDMTMS5_07 | 82.6 | 85.3 | 84.0 | |
| 5.0 | EDMTMS5_08 | 86.6 | 88.6 | 87.6 | |
| 5.0 | EDMTMS5_09 | 85.2 | 86.5 | 85.9 | 3.2 |
| 5.0 | EDMTMS5_10 | 86.8 | 86.1 | 86.5 | 2.5 |
| **5.0** | **AVERAGE** | **87.0** | **87.7** | **87.4** | 2.8 |
| 6.0 | EDMTMS6_01 | 81.7 | 82.7 | 82.2 | |
| 6.0 | EDMTMS6_02 | 99.6 | 99.2 | 99.4 | |
| 6.0 | EDMTMS6_03 | 86.1 | 90.0 | 88.1 | |
| 6.0 | EDMTMS6_04 | 95.1 | 94.7 | 94.9 | |
| 6.0 | EDMTMS6_05 | 88.0 | 85.6 | 86.8 | |
| 6.0 | EDMTMS6_06 | 88.8 | 90.5 | 89.6 | |
| 6.0 | EDMTMS6_07 | 84.9 | 86.9 | 85.9 | |
| 6.0 | EDMTMS6_08 | 94.5 | 94.8 | 94.7 | |
| 6.0 | EDMTMS6_09 | 92.4 | 88.7 | 90.6 | 6.1 |
| 6.0 | EDMTMS6_10 | 79.5 | 81.7 | 80.6 | 5.4 |
| **6.0** | **AVERAGE** | **89.9** | **90.2** | **90.1** | 5.9 |
| 7.0 | EDMTMS7_01 | 84.3 | 74.7 | 79.5 | |
| 7.0 | EDMTMS7_02 | 92.7 | 96.1 | 94.4 | |
| 7.0 | EDMTMS7_03 | 107.1 | 104.8 | 106.0 | |
| 7.0 | EDMTMS7_04 | 106.8 | 105.7 | 106.3 | |
| 7.0 | EDMTMS7_05 | 105.8 | 103.1 | 104.5 | |
| 7.0 | EDMTMS7_06 | 101.6 | 100.5 | 101.1 | |
| 7.0 | EDMTMS7_07 | 114.8 | 114.1 | 114.5 | |

| | | | | | |
|---|---|---|---|---|---|
| 7.0 | EDMTMS7_08 | 101.9 | 102.2 | 102.1 | |
| 7.0 | EDMTMS7_09 | 94.7 | 97.5 | 96.1 | 8.7 |
| 7.0 | EDMTMS7_10 | 103.9 | 102.2 | 103.1 | 10.2 |
| **7.0** | **AVERAGE** | **101.4** | **100.1** | **100.7** | 9.3 |
| 8.0 | EDMTMS8_01 | 153.0 | 135.5 | 144.3 | |
| 8.0 | EDMTMS8_02 | 136.0 | 134.8 | 135.4 | |
| 8.0 | EDMTMS8_03 | 128.4 | 128.1 | 128.3 | |
| 8.0 | EDMTMS8_04 | 135.7 | 135.5 | 135.6 | |
| 8.0 | EDMTMS8_05 | 130.0 | 130.1 | 130.1 | |
| 8.0 | EDMTMS8_06 | 125.5 | 128.3 | 126.9 | |
| 8.0 | EDMTMS8_07 | 136.3 | 136.4 | 136.4 | |
| 8.0 | EDMTMS8_08 | 132.4 | 133.2 | 132.8 | |
| 8.0 | EDMTMS8_09 | 148.9 | 143.9 | 146.4 | 7.7 |
| 8.0 | EDMTMS8_10 | 122.8 | 124.7 | 123.8 | 5.7 |
| **8.0** | **AVERAGE** | **132.9** | **132.8** | **132.8** | 7.3 |
| 9.0 | EDMTMS9_01 | 101.0 | 101.2 | 101.1 | |
| 9.0 | EDMTMS9_02 | 106.7 | 108.3 | 107.5 | |
| 9.0 | EDMTMS9_03 | 85.1 | 87.9 | 86.5 | |
| 9.0 | EDMTMS9_04 | 106.7 | 105.1 | 105.9 | |
| 9.0 | EDMTMS9_05 | 108.3 | 109.8 | 109.1 | |
| 9.0 | EDMTMS9_06 | 112.2 | 115.0 | 113.6 | |
| 9.0 | EDMTMS9_07 | 120.9 | 121.0 | 121.0 | |
| 9.0 | EDMTMS9_08 | 118.9 | 118.5 | 118.7 | |
| 9.0 | EDMTMS9_09 | 116.0 | 118.6 | 117.3 | 12.1 |
| 9.0 | EDMTMS9_10 | 129.0 | 129.2 | 129.1 | 11.7 |
| **9.0** | **AVERAGE** | **110.5** | **111.5** | **111.0** | 11.9 |
| 10.0 | EDMTMS10_01 | 108.3 | 108.5 | 108.4 | |
| 10.0 | EDMTMS10_02 | 130.6 | 130.4 | 130.5 | |
| 10.0 | EDMTMS10_03 | 147.8 | 147.8 | 147.8 | |
| 10.0 | EDMTMS10_04 | 117.3 | 117.0 | 117.2 | |
| 10.0 | EDMTMS10_05 | 138.4 | 137.6 | 138.0 | |
| 10.0 | EDMTMS10_06 | 140.2 | 133.0 | 136.6 | |
| 10.0 | EDMTMS10_07 | 110.2 | 111.3 | 110.8 | |
| 10.0 | EDMTMS10_08 | 146.9 | 146.8 | 146.9 | |
| 10.0 | EDMTMS10_09 | 132.6 | 131.1 | 131.9 | 14.7 |
| 10.0 | EDMTMS10_10 | 117.9 | 119.1 | 118.5 | 13.9 |
| **10.0** | **AVERAGE** | **129.0** | **128.3** | **128.6** | 14.3 |
| 11.0 | EDMTMS11_01 | 109.8 | 107.9 | 108.9 | |
| 11.0 | EDMTMS11_02 | 107.2 | 105.5 | 106.4 | |
| 11.0 | EDMTMS11_03 | 104.7 | 105.8 | 105.3 | |

| | | | | | |
|---|---|---|---|---|---|
| 11.0 | EDMTMS11_04 | 116.5 | 111.7 | 114.1 | |
| 11.0 | EDMTMS11_05 | 105.3 | 100.7 | 103.0 | |
| 11.0 | EDMTMS11_06 | 94.3 | 94.4 | 94.4 | |
| 11.0 | EDMTMS11_07 | 105.7 | 109.7 | 107.7 | |
| 11.0 | EDMTMS11_08 | 105.7 | 105.8 | 105.8 | |
| 11.0 | EDMTMS11_09 | 101.4 | 102.1 | 101.8 | 6.3 |
| 11.0 | EDMTMS11_10 | 96.4 | 97.8 | 97.1 | 5.4 |
| **11.0** | **AVERAGE** | **104.7** | **104.1** | **104.4** | 5.7 |
| 12.0 | EDMTMS12_01 | 54.7 | 52.1 | 53.4 | |
| 12.0 | EDMTMS12_02 | 52.6 | 51.4 | 52.0 | |
| 12.0 | EDMTMS12_03 | 61.4 | 62.7 | 62.1 | |
| 12.0 | EDMTMS12_04 | 54.2 | 52.2 | 53.2 | |
| 12.0 | EDMTMS12_05 | 55.8 | 50.6 | 53.2 | |
| 12.0 | EDMTMS12_06 | 45.2 | 46.6 | 45.9 | |
| 12.0 | EDMTMS12_07 | 61.5 | 63.6 | 62.6 | |
| 12.0 | EDMTMS12_08 | 57.0 | 55.7 | 56.4 | |
| 12.0 | EDMTMS12_09 | 55.5 | 59.6 | 57.6 | 4.9 |
| 12.0 | EDMTMS12_10 | 49.7 | 48.5 | 49.1 | 5.9 |
| **12.0** | **AVERAGE** | **54.8** | **54.3** | **54.5** | 5.3 |
| 8.0 | EDMTMS08_11 | 143.8 | 143.8 | 143.8 | |
| 8.0 | EDMTMS08_12 | 124.4 | 125.0 | 124.7 | |
| 8.0 | EDMTMS08_13 | 145.8 | 144.8 | 145.3 | |
| 8.0 | EDMTMS08_14 | 128.1 | 129.3 | 128.7 | |
| 8.0 | EDMTMS08_15 | 132.7 | 132.7 | 132.7 | |
| 8.0 | EDMTMS08_16 | 140.4 | 141.7 | 141.1 | |
| 8.0 | EDMTMS08_17 | 148.4 | 148.5 | 148.5 | |
| 8.0 | EDMTMS08_18 | 136.0 | 136.3 | 136.2 | |
| 8.0 | EDMTMS08_19 | 131.9 | 132.2 | 132.1 | 7.9 |
| 8.0 | EDMTMS08_20 | 141.4 | 141.7 | 141.6 | 7.6 |
| **8.0** | **AVERAGE** | **137.3** | **137.6** | **137.4** | **7.8** |
| 10.0 | EDMTMS10_11 | 137.9 | 138.4 | 138.2 | |
| 10.0 | EDMTMS10_12 | 119.0 | 118.8 | 118.9 | |
| 10.0 | EDMTMS10_13 | 127.2 | 127.3 | 127.3 | |
| 10.0 | EDMTMS10_14 | 138.6 | 138.5 | 138.6 | |
| 10.0 | EDMTMS10_15 | 106.4 | 110.3 | 108.4 | |
| 10.0 | EDMTMS10_16 | 115.6 | 117.8 | 116.7 | |
| 10.0 | EDMTMS10_17 | 114.9 | 115.6 | 115.3 | |
| 10.0 | EDMTMS10_18 | 117.6 | 117.9 | 117.8 | |
| 10.0 | EDMTMS10_19 | 131.9 | 108.1 | 106.6 | 11.7 |
| 10.0 | EDMTMS10_20 | 107.3 | 105.7 | 106.5 | 11.6 |

| | | | | | |
|---|---|---|---|---|---|
| **8.0** | **AVERAGE** | **121.6** | **119.8** | **119.4** | **11.8** |

**Table A.2** Contact Angles for slides made in Multilevel Factorial Design
(Cells highlighted in blue were taken after water testing.)

| Experiment # | FILE NAME | CA Left | CA Right | Average | Std Dev |
|---|---|---|---|---|---|
| 5-3 | EDMTMS_5-3_01 | 112.6 | 112.6 | 112.6 | |
| 5-3 | EDMTMS_5-3_02 | 113.5 | 113.5 | 113.5 | |
| 5-3 | EDMTMS_5-3_03 | 96.1 | 96.1 | 96.1 | |
| 5-3 | EDMTMS_5-3_04 | 115.9 | 115.9 | 115.9 | |
| 5-3 | EDMTMS_5-3_05 | 111.1 | 109.9 | 110.5 | |
| 5-3 | EDMTMS_5-3_06 | 97.3 | 95.4 | 96.4 | |
| 5-3 | EDMTMS_5-3_07 | 119.9 | 117.7 | 118.8 | |
| 5-3 | EDMTMS_5-3_08 | 97.7 | 98.3 | 98.0 | |
| 5-3 | EDMTMS_5-3_09 | 110.0 | 107.9 | 109.0 | 12.5 |
| 5-3 | EDMTMS_5-3_10 | 137.6 | 131.4 | 134.5 | 11.1 |
| 5-3 | **AVERAGE** | **111.2** | **109.9** | **110.5** | 11.8 |
| 5-5 | EDMTMS_5-5_01 | 96.5 | 98.7 | 97.6 | |
| 5-5 | EDMTMS_5-5_02 | 121.5 | 123.4 | 122.5 | |
| 5-5 | EDMTMS_5-5_03 | 118.4 | 119.9 | 119.2 | |
| 5-5 | EDMTMS_5-5_04 | 107.1 | 108.0 | 107.6 | |
| 5-5 | EDMTMS_5-5_05 | 99.0 | 99.0 | 99.0 | |
| 5-5 | EDMTMS_5-5_06 | 115.3 | 115.3 | 115.3 | |
| 5-5 | EDMTMS_5-5_07 | 148.6 | 150.0 | 149.3 | |
| 5-5 | EDMTMS_5-5_08 | 126.5 | 126.1 | 126.3 | |
| 5-5 | EDMTMS_5-5_09 | 85.2 | 85.2 | 85.2 | 18.1 |
| 5-5 | EDMTMS_5-5_10 | 102.5 | 101.0 | 101.8 | 18.4 |
| 5-5 | **AVERAGE** | **112.1** | **112.7** | **112.4** | 18.2 |
| 5-7 | EDMTMS_5-7_01 | 122.0 | 122.1 | 122.1 | |
| 5-7 | EDMTMS_5-7_02 | 137.7 | 137.0 | 137.4 | |
| 5-7 | EDMTMS_5-7_03 | 115.3 | 114.0 | 114.7 | |
| 5-7 | EDMTMS_5-7_04 | 118.5 | 115.2 | 116.9 | |
| 5-7 | EDMTMS_5-7_05 | 142.1 | 145.1 | 143.6 | |
| 5-7 | EDMTMS_5-7_06 | 115.5 | 113.3 | 114.4 | |
| 5-7 | EDMTMS_5-7_07 | 102.5 | 103.7 | 103.1 | |
| 5-7 | EDMTMS_5-7_08 | 109.0 | 109.0 | 109.0 | |
| 5-7 | EDMTMS_5-7_09 | 143.7 | 144.7 | 144.2 | 14.7 |
| 5-7 | EDMTMS_5-7_10 | 109.2 | 108.3 | 108.8 | 15.4 |
| 5-7 | **AVERAGE** | **121.6** | **121.2** | **121.4** | 15.0 |
| 10-3 | EDMTMS_10-3_01 | 153.5 | 153.1 | 153.3 | |
| 10-3 | EDMTMS_10-3_02 | 107.6 | 108.6 | 108.1 | |
| 10-3 | EDMTMS_10-3_03 | 108.1 | 108.1 | 108.1 | |

| | | | | | |
|---|---|---|---|---|---|
| 10-3 | EDMTMS_10-3_04 | 123.2 | 123.4 | 123.3 | |
| 10-3 | EDMTMS_10-3_05 | 148.9 | 145.4 | 147.2 | |
| 10-3 | EDMTMS_10-3_06 | 116.3 | 119.1 | 117.7 | |
| 10-3 | EDMTMS_10-3_07 | 106.5 | 106.5 | 106.5 | |
| 10-3 | EDMTMS_10-3_08 | 105.9 | 109.0 | 107.5 | |
| 10-3 | EDMTMS_10-3_09 | 93.0 | 90.5 | 91.8 | 21.0 |
| 10-3 | EDMTMS_10-3_10 | 144.6 | 143.6 | 144.1 | 20.4 |
| 10-3 | **AVERAGE** | **120.8** | **120.7** | **120.7** | 20.7 |
| 10-5 | EDMTMS_10-5_01 | 164.8 | 164.6 | 164.7 | |
| 10-5 | EDMTMS_10-5_02 | 111.2 | 114.0 | 112.6 | |
| 10-5 | EDMTMS_10-5_03 | 155.4 | 156.5 | 156.0 | |
| 10-5 | EDMTMS_10-5_04 | 118.0 | 105.2 | 111.6 | |
| 10-5 | EDMTMS_10-5_05 | 104.2 | 103.8 | 104.0 | |
| 10-5 | EDMTMS_10-5_06 | 119.5 | 124.4 | 122.0 | |
| 10-5 | EDMTMS_10-5_07 | 88.9 | 100.8 | 94.9 | |
| 10-5 | EDMTMS_10-5_08 | 117.4 | 116.0 | 116.7 | |
| 10-5 | EDMTMS_10-5_09 | 147.0 | 150.2 | 148.6 | 24.4 |
| 10-5 | EDMTMS_10-5_10 | 107.3 | 107.3 | 107.3 | 23.9 |
| 10-5 | **AVERAGE** | **123.4** | **124.3** | **123.8** | 23.9 |
| 10-7 | EDMTMS_10-7_01 | 96.0 | 91.2 | 93.6 | |
| 10-7 | EDMTMS_10-7_02 | 111.8 | 109.8 | 110.8 | |
| 10-7 | EDMTMS_10-7_03 | 118.1 | 120.4 | 119.3 | |
| 10-7 | EDMTMS_10-7_04 | 97.9 | 97.9 | 97.9 | |
| 10-7 | EDMTMS_10-7_05 | 136.8 | 136.7 | 136.8 | |
| 10-7 | EDMTMS_10-7_06 | 152.2 | 154.7 | 153.5 | |
| 10-7 | EDMTMS_10-7_07 | 118.4 | 124.1 | 121.3 | |
| 10-7 | EDMTMS_10-7_08 | 92.8 | 92.8 | 92.8 | |
| 10-7 | EDMTMS_10-7_09 | 116.5 | 116.5 | 116.5 | 18.4 |
| 10-7 | EDMTMS_10-7_10 | 118.8 | 121.9 | 120.4 | 19.9 |
| 10-7 | **AVERAGE** | **115.9** | **116.6** | **116.3** | 19.1 |
| 15-3 | EDMTMS_15-3_01 | 118.0 | 117.1 | 117.6 | |
| 15-3 | EDMTMS_15-3_02 | 128.3 | 135.6 | 132.0 | |
| 15-3 | EDMTMS_15-3_03 | 133.9 | 134.2 | 134.1 | |
| 15-3 | EDMTMS_15-3_04 | 137.0 | 138.5 | 137.8 | |
| 15-3 | EDMTMS_15-3_05 | 135.0 | 133.0 | 134.0 | |
| 15-3 | EDMTMS_15-3_06 | 143.9 | 144.1 | 144.0 | |
| 15-3 | EDMTMS_15-3_07 | 135.2 | 135.2 | 135.2 | |
| 15-3 | EDMTMS_15-3_08 | 143.2 | 143.2 | 143.2 | |
| 15-3 | EDMTMS_15-3_09 | 140.0 | 139.4 | 139.7 | 9.9 |
| 15-3 | EDMTMS_15-3_10 | 114.5 | 112.7 | 113.6 | 10.4 |

| | | | | | |
|---|---|---|---|---|---|
| 15-3 | **AVERAGE** | **132.9** | **133.3** | **133.1** | 10.1 |
| 15-5 | EDMTMS_15-5_01 | 135.3 | 135.3 | 135.3 | |
| 15-5 | EDMTMS_15-5_02 | 123.7 | 125.7 | 124.7 | |
| 15-5 | EDMTMS_15-5_03 | 138.6 | 138.6 | 138.6 | |
| 15-5 | EDMTMS_15-5_04 | 110.5 | 113.1 | 111.8 | |
| 15-5 | EDMTMS_15-5_05 | 143.2 | 142.4 | 142.8 | |
| 15-5 | EDMTMS_15-5_06 | 142.3 | 142.0 | 142.2 | |
| 15-5 | EDMTMS_15-5_07 | 132.8 | 134.1 | 133.5 | |
| 15-5 | EDMTMS_15-5_08 | 133.3 | 139.3 | 136.3 | |
| 15-5 | EDMTMS_15-5_09 | 121.0 | 113.7 | 117.4 | 10.9 |
| 15-5 | EDMTMS_15-5_10 | 118.9 | 118.9 | 118.9 | 11.5 |
| 15-5 | **AVERAGE** | **130.0** | **130.3** | **130.1** | 11.1 |
| 15-7 | EDMTMS_15-7_01 | 108.5 | 103.7 | 106.1 | |
| 15-7 | EDMTMS_15-7_02 | 138.5 | 137.7 | 138.1 | |
| 15-7 | EDMTMS_15-7_03 | 118.8 | 118.8 | 118.8 | |
| 15-7 | EDMTMS_15-7_04 | 123.1 | 127.0 | 125.1 | |
| 15-7 | EDMTMS_15-7_05 | 131.7 | 133.9 | 132.8 | |
| 15-7 | EDMTMS_15-7_06 | 141.0 | 141.9 | 141.5 | |
| 15-7 | EDMTMS_15-7_07 | 144.2 | 142.6 | 143.4 | |
| 15-7 | EDMTMS_15-7_08 | 128.5 | 128.5 | 128.5 | |
| 15-7 | EDMTMS_15-7_09 | 150.0 | 150.2 | 150.1 | 13.5 |
| 15-7 | EDMTMS_15-7_10 | 147.8 | 146.5 | 147.2 | 14.1 |
| 15-7 | **AVERAGE** | **133.2** | **133.1** | **133.1** | 13.8 |
| 10-5 | EDMTMS_10-5_11 | 96.9 | 96.9 | 96.9 | |
| 10-5 | EDMTMS_10-5_12 | 130.3 | 126.6 | 128.5 | |
| 10-5 | EDMTMS_10-5_13 | 111.1 | 111.1 | 111.1 | |
| 10-5 | EDMTMS_10-5_14 | 102.9 | 104.6 | 103.8 | |
| 10-5 | EDMTMS_10-5_15 | 112.5 | 113.0 | 112.8 | |
| 10-5 | EDMTMS_10-5_16 | 136.8 | 133.4 | 135.1 | |
| 10-5 | EDMTMS_10-5_17 | 102.3 | 112.1 | 107.2 | |
| 10-5 | EDMTMS_10-5_18 | 118.5 | 123.9 | 121.2 | |
| 10-5 | EDMTMS_10-5_19 | 91.0 | 87.2 | 89.1 | 14.3 |
| 10-5 | EDMTMS_10-5_20 | 109.1 | 107.9 | 108.5 | 13.9 |
| 10-5 | **AVERAGE** | **111.1** | **111.7** | **111.4** | 13.9 |
| 15-5 | EDMTMS_15-5_11 | 147.7 | 147.0 | 147.4 | |
| 15-5 | EDMTMS_15-5_12 | 129.1 | 126.7 | 127.9 | |
| 15-5 | EDMTMS_15-5_13 | 98.1 | 98.1 | 98.1 | |
| 15-5 | EDMTMS_15-5_14 | 106.9 | 107.4 | 107.2 | |
| 15-5 | EDMTMS_15-5_15 | 130.5 | 124.4 | 127.5 | |
| 15-5 | EDMTMS_15-5_16 | 109.9 | 119.1 | 114.5 | |

| | | | | | |
|---|---|---|---|---|---|
| 15-5 | EDMTMS_15-5_17 | 107.7 | 111.4 | 109.6 | |
| 15-5 | EDMTMS_15-5_18 | 140.4 | 142.9 | 141.7 | |
| 15-5 | EDMTMS_15-5_19 | 129.4 | 128.6 | 129.0 | 17.1 |
| 15-5 | EDMTMS_15-5_20 | 140.8 | 139.2 | 140.0 | 15.9 |
| 15-5 | **AVERAGE** | **124.1** | **124.5** | **124.3** | 16.4 |

**Table A.3** Contact Angles for slides made in using procedure 1

| Experiment # | FILE NAME | CA Left | CA Right | Average | Std Dev |
|---|---|---|---|---|---|
| R1-01 | EDMTMSR1-01_01 | 145.5 | 145.3 | 145.4 | |
| R1-01 | EDMTMSR1-01_02 | 133.5 | 134.9 | 134.2 | |
| R1-01 | EDMTMSR1-01_03 | 149.3 | 147.1 | 148.2 | |
| R1-01 | EDMTMSR1-01_04 | 114.2 | 111.2 | 112.7 | |
| R1-01 | EDMTMSR1-01_05 | 108.2 | 108.2 | 108.2 | |
| R1-01 | EDMTMSR1-01_06 | 133.7 | 132.1 | 132.9 | |
| R1-01 | EDMTMSR1-01_07 | 100.7 | 101.2 | 101.0 | |
| R1-01 | EDMTMSR1-01_08 | 100.7 | 98.6 | 99.7 | |
| R1-01 | EDMTMSR1-01_09 | 120.7 | 116.3 | 118.5 | 17.7 |
| R1-01 | EDMTMSR1-01_10 | 113.2 | 118.2 | 115.7 | 17.5 |
| R1-01 | **Average** | 122.0 | 121.3 | 121.6 | 17.5 |
| R1-02 | EDMTMSR1-02_01 | 108.0 | 108.8 | 108.4 | |
| R1-02 | EDMTMSR1-02_02 | 126.2 | 124.3 | 125.3 | |
| R1-02 | EDMTMSR1-02_03 | 103.3 | 108.6 | 106.0 | |
| R1-02 | EDMTMSR1-02_04 | 105.3 | 110.3 | 107.8 | |
| R1-02 | EDMTMSR1-02_05 | 107.1 | 111.1 | 109.1 | |
| R1-02 | EDMTMSR1-02_06 | 123.4 | 126.5 | 125.0 | |
| R1-02 | EDMTMSR1-02_07 | 133.4 | 132.2 | 132.8 | |
| R1-02 | EDMTMSR1-02_08 | 91.6 | 90.8 | 91.2 | |
| R1-02 | EDMTMSR1-02_09 | 145.4 | 145.9 | 145.7 | 16.6 |
| R1-02 | EDMTMSR1-02_10 | 128.5 | 128.6 | 128.6 | 15.7 |
| R1-02 | **Average** | 117.2 | 118.7 | 118.0 | 16.1 |
| R1-03 | EDMTMSR1-03_01 | 144.1 | 143.1 | 143.6 | |
| R1-03 | EDMTMSR1-03_02 | 95.9 | 96.5 | 96.2 | |
| R1-03 | EDMTMSR1-03_03 | 125.9 | 126.2 | 126.1 | |
| R1-03 | EDMTMSR1-03_04 | 109.2 | 106.7 | 108.0 | |
| R1-03 | EDMTMSR1-03_05 | 117.2 | 120.5 | 118.9 | |
| R1-03 | EDMTMSR1-03_06 | 101.0 | 101.3 | 101.2 | |
| R1-03 | EDMTMSR1-03_07 | 112.6 | 114.4 | 113.5 | |
| R1-03 | EDMTMSR1-03_08 | 94.1 | 92.5 | 93.3 | |
| R1-03 | EDMTMSR1-03_09 | 95.3 | 96.5 | 95.9 | 15.7 |
| R1-03 | EDMTMSR1-03_10 | 107.3 | 109.4 | 108.4 | 15.8 |
| R1-03 | **Average** | 110.3 | 110.7 | 110.5 | 15.7 |

| | | | | | |
|---|---|---|---|---|---|
| R1-04 | EDMTMSR1-04_01 | 116.3 | 116.4 | 116.4 | |
| R1-04 | EDMTMSR1-04_02 | 133.7 | 136.6 | 135.2 | |
| R1-04 | EDMTMSR1-04_03 | 141.0 | 138.5 | 139.8 | |
| R1-04 | EDMTMSR1-04_04 | 125.7 | 125.8 | 125.8 | |
| R1-04 | EDMTMSR1-04_05 | 137.4 | 138.1 | 137.8 | |
| R1-04 | EDMTMSR1-04_06 | 120.6 | 121.0 | 120.8 | |
| R1-04 | EDMTMSR1-04_07 | 114.1 | 117.2 | 115.7 | |
| R1-04 | EDMTMSR1-04_08 | 125.4 | 125.4 | 125.4 | |
| R1-04 | EDMTMSR1-04_09 | 127.9 | 129.0 | 128.5 | 8.8 |
| R1-04 | EDMTMSR1-04_10 | 122.5 | 119.8 | 121.2 | 8.5 |
| R1-04 | **Average** | 126.5 | 126.8 | 126.6 | 8.6 |
| R1-05 | EDMTMSR1-05_01 | 96.7 | 102.5 | 99.6 | |
| R1-05 | EDMTMSR1-05_02 | 104.9 | 103.4 | 104.2 | |
| R1-05 | EDMTMSR1-05_03 | 132.8 | 134.1 | 133.5 | |
| R1-05 | EDMTMSR1-05_04 | 128.7 | 128.8 | 128.8 | |
| R1-05 | EDMTMSR1-05_05 | 106.2 | 107.5 | 106.9 | |
| R1-05 | EDMTMSR1-05_06 | 103.2 | 101.2 | 102.2 | |
| R1-05 | EDMTMSR1-05_07 | 102.5 | 101.1 | 101.8 | |
| R1-05 | EDMTMSR1-05_08 | 116.0 | 115.7 | 115.9 | |
| R1-05 | EDMTMSR1-05_09 | 101.6 | 102.6 | 102.1 | 13.1 |
| R1-05 | EDMTMSR1-05_10 | 126.6 | 127.2 | 126.9 | 13.0 |
| R1-05 | **Average** | 111.9 | 112.4 | 112.2 | 13.0 |

**Table A.4** Contact Angles for slides made in using RSCE recipe

| Experiment # | FILE NAME | CA Left | CA Right | Average | Std Dev |
|---|---|---|---|---|---|
| TMOS 50 MTMS | EDTMOS50MTMS_01 | 95.4 | 96.0 | 95.7 | |
| TMOS 50 MTMS | EDTMOS50MTMS_02 | 91.7 | 91.7 | 91.7 | |
| TMOS 50 MTMS | EDTMOS50MTMS_03 | 66.3 | 64.4 | 65.4 | |
| TMOS 50 MTMS | EDTMOS50MTMS_04 | 78.7 | 77.4 | 78.1 | |
| TMOS 50 MTMS | EDTMOS50MTMS_05 | 88.9 | 90.7 | 89.8 | |
| TMOS 50 MTMS | EDTMOS50MTMS_06 | 114.4 | 115.4 | 114.9 | |
| TMOS 50 MTMS | EDTMOS50MTMS_07 | 92.9 | 94.6 | 93.8 | |
| TMOS 50 MTMS | EDTMOS50MTMS_08 | 100.3 | 98.5 | 99.4 | |
| TMOS 50 MTMS | EDTMOS50MTMS_09 | 103.5 | 100.9 | 102.2 | 13.3 |
| TMOS 50 MTMS | EDTMOS50MTMS_10 | 97.3 | 100.0 | 98.7 | 13.8 |
| TMOS 50 MTMS | **Average** | 92.9 | 93.0 | 93.0 | 13.5 |
| TMOS 25 MTMS | EDTMOS25MTMS_01 | 77.9 | 78.1 | 78.0 | |
| TMOS 25 MTMS | EDTMOS25MTMS_02 | 83.5 | 74.4 | 79.0 | |
| TMOS 25 MTMS | EDTMOS25MTMS_03 | 88.9 | 84.9 | 86.9 | |
| TMOS 25 MTMS | EDTMOS25MTMS_04 | 78.2 | 76.1 | 77.2 | |
| TMOS 25 MTMS | EDTMOS25MTMS_05 | 89.8 | 82.9 | 86.4 | |

| | | | | | |
|---|---|---|---|---|---|
| TMOS 25 MTMS | EDTMOS25MTMS_06 | 91.7 | 91.6 | 91.7 | |
| TMOS 25 MTMS | EDTMOS25MTMS_07 | 51.9 | 51.7 | 51.8 | |
| TMOS 25 MTMS | EDTMOS25MTMS_08 | 81.2 | 78.0 | 79.6 | |
| TMOS 25 MTMS | EDTMOS25MTMS_09 | 73.8 | 74.2 | 74.0 | 13.1 |
| TMOS 25 MTMS | EDTMOS25MTMS_10 | 59.0 | 57.8 | 58.4 | 12.0 |
| TMOS 25 MTMS | **Average** | 77.6 | 75.0 | 76.3 | 12.5 |